

Impulse response estimation via flexible local projections *

Haroon Mumtaz[†] Michele Piffer[‡]

November 23, 2025

Abstract

This paper introduces a flexible local projection that generalises the model by Jordà (2005) to a non-parametric setting using Bayesian Additive Regression Trees. Monte Carlo experiments show that the BART-LP model captures multiple types of non-linearities in the impulse responses within the same framework. Our first application shows that adverse financial shocks generate effects that increase more than proportionately in the size of the shock, explaining the large economic effects of strong financial disruptions. Our second application shows that before Covid-19 monetary policy shocks were more effective during economic expansions if they were contractionary shocks, while expansionary shocks generate symmetric effects.

JEL classification: C14, C11, C32, E52.

Keywords: Non-linear models, non-parametric techniques.

*We are thankful to Luca Neri and Vito Polito for helpful comments and suggestions. The views expressed in this paper are those of the authors and do not necessarily represent the views of the Bank of England or its committees.

[†]Queen Mary, University of London, School of Economics and Finance, Mile End road, London E1 4LJ, UK. e-mail: h.mumtaz@qmul.ac.uk

[‡]Bank of England, Threadneedle St, City of London, London EC2R 8AH, UK, and King's Business School, King's College London, Bush House, 30 Aldwych, London WC2B 4BG, UK. e-mail: m.b.piffer@gmail.com

1 Introduction

Estimation of impulse responses (IRFs) via local projections (LP) by [Jordà \(2005\)](#) has become increasingly common in applied Macroeconometric analysis. A key feature of the local projection estimator is that it estimates IRFs of variable y_t to an innovation to variable x_t directly via linear regressions of the form $y_{t+h} = \beta_h x_t + d_h \mathbf{w}_t + u_{t+h}$, where \mathbf{w}_t denotes control variables. Given their flexibility, considerable attention has been given to investigate the properties of the LP estimator, see, for instance, [Stock and Watson \(2018\)](#) and [Plagborg-Møller and Wolf \(2021\)](#).

In their most popular specification, LP estimators impose a linearity between y_{t+h} and (x_t, \mathbf{w}_t) . This limitation implies that linear LPs cannot be used to study non-linear effects of the shocks of interest, for instance non-linearities on the sign or size of the shock, or on the economic conditions when the shock occurs. Some extensions of the linear LP estimator have been proposed, but they all rely on the functional form introduced to model the non-linearity. [Jordà \(2005\)](#) proposes the use of quadratic and cubic terms. [Auerbach and Gorodnichenko \(2013a,b\)](#) and [Ramey and Zubairy \(2018\)](#) use a smooth transition function and a threshold function, respectively. [Ruisi \(2019\)](#) and [Lusompa \(2023\)](#) use a time varying extension of LP based on parametric state-space models, while [Inoue et al. \(2024\)](#) provides a more general framework for modelling structural shifts. Most of the parametric non-linear LP estimators can only study one non-linearity at a time, hence failing to offer a unified framework where multiple non-linearities can potentially interact. In addition, [Gonçalves et al. \(2022\)](#) document that nonlinear parametric LP estimators can fail to consistently estimate the true conditional average response of interest when the nonlinearity is endogenous to the system.

In this paper we propose a flexible non-linear extension of the LP estimator that does not require assumptions on the functional form of the LP regression equation, and that allows for multiple types of non-linearities. We propose a non-parametric LP estimator that uses the Bayesian Additive Regression Trees (BART) model to approxi-

mate the unknown function $m_h(\mathbf{z}_t)$ in the more general equation $y_{t+h} = m_h(\mathbf{z}_t) + u_{t+h}$, with $\mathbf{z}_t = (x_t, \mathbf{w}_t)$. Introduced by Chipman et al. (2010), BART uses regression trees as its building block. Regression trees split the space of explanatory variables \mathbf{z}_t into sub-groups based on binary rules. The function $m_h(\mathbf{z}_t)$ is approximated as a sum of a large number of small trees. Chipman et al. (2010) show that BART is able to approximate highly non-linear functions accurately.

We first illustrate how BART techniques can be applied in a non-linear LP estimator, and we refer to this new methodology as BART-LP. We show that BART-LP can handle autocorrelation in the error terms, a problem already discussed in the literature of linear LP estimators. We then document the performance of BART-LP using Monte Carlo analysis. We build our simulations on three models. First, we use the same SVAR-GARCH model employed in the simulation by Jordà (2005), where a structural shock generates non-linear effects that affect the variance of the shock. Second, we use a sign-dependent moving average model in which the true monetary policy shock generates different effects depending on the sign of the shock. Third, we use a recursive Threshold VAR model in which shocks generate stronger effects in one of the two regimes of the model, where the transition across regimes is endogenous to the system. We show that the same BART-LP methodology can recover the true impulse responses in all non-linear models considered. We also show that the BART-LP methodology works well in an environment in which the data generating process is linear. We focus the discussion on the IRF estimation, which is separate from identification of the structural shocks. As also in Jordà (2005), we do not investigate the topic of identification in our framework.

We apply our methodology to study whether financial shocks can generate strong and persistent effects on the real economy in the US. To the best of our knowledge, Forni et al. (2024) are the first to propose a model that can jointly capture the potential non-linear effects of financial shocks over the size and sign of the shock. Their model is parametric, and uses a cubic functional form that constrains how these non-linearities

enter the model. We use the flexible BART-LP methodology to document two main findings. First, we show that, as in [Forni et al. \(2024\)](#), adverse financial shocks generate effects that increase more than proportionately in the size of the shock. Second, we show that the parametric constraints introduced by [Forni et al. \(2024\)](#) cannot detect that the increase in the size of the shock also changes the timing of the response, speeding up the contractionary response of the real economy. This finding helps understand why unprecedented large financial disruptions (for instance the 2007 financial crisis) can generate deep recessions that are hard to predict using linear models based on previous financial events. We show that the results are robust to the inclusion of data from the Covid period. The analysis is part of a broader literature, see, for instance, by [Gilchrist and Zakrajsek \(2012\)](#), [Romer and Romer \(2017\)](#) and [Barnichon, Matthes and Ziegenbein \(2022\)](#).

We then apply our methodology to shed light on the debate on how effective monetary policy shocks are depending on the state of the economy when the shock occurs. While the smooth transition VAR model by [Weise \(1999\)](#) documents that monetary policy shocks are more effective in economic recessions, the smooth transition LP model by [Tenreyro and Thwaites \(2016\)](#) finds the opposite result. Neither model is explicitly designed to jointly study non-linearities not only on the state of the economy, but also over the size and the sign of the monetary stimulus. We use BART-LP to document that whether a monetary policy shock is more effective in economic expansion or recessions depends on the sign of the shock and on the sample period. Before Covid, contractionary shocks are found to be considerably more effective in economic expansions (as in [Tenreyro and Thwaites, 2016](#)), while expansionary shocks generate stronger effects in recession (as in [Weise, 1999](#)). We also find that for contractionary shocks, the effects increase more than proportionately as the size of the shock increases. The results are consistent with the models by [Barnichon and Matthes \(2018\)](#), [Alessandri et al. \(2022\)](#) and [Bruns and Piffer \(2023\)](#), who nevertheless do not study multiple non-linearities within a unified framework. These contributions do not

include Covid. We document that the nonlinearity is mostly attenuated when post Covid data is used in the analysis.

This paper relates to the literature that studies how BART techniques can be used in Macroeconomics. Prüser (2019) uses BART on a large set of univariate time series models to show that BART offers a highly competitive tool for forecasting. Huber and Rossini (2022) introduce a VAR model where the dynamics of the endogenous variables are modelled using BART. The authors model the impact of uncertainty shocks using their proposed model. Huber et al. (2023) extend the BART-VAR to a mixed frequency setting and evaluate the forecasting performance of the model. Clark et al. (2023) show that multivariate BART regression models perform well in terms of tail forecasting. To the best of our knowledge, our paper is the first one to use BART in an LP framework. The paper is also part of a broad literature that studies the advantages of IRF estimation using LP estimators, relative to constructing IRFs on vector autoregressive models. Several contributions document the performance of LP estimators, including Gonçalves et al. (2022), Kilian and Kim (2011), Alloza et al. (2025), Breitung and Brüggemann (2023) Herbst and Johannsen (2024), Li et al. (2024) and Bruns and Lütkepohl (2022). While LP estimators are usually proposed in a frequentist setting, we follow Ferreira et al. (2023a) and take a Bayesian approach to LP, yet in a non-linear framework. In a closely related paper, Paranhos (2022) proposes a non-linear LP where the non-linearity is captured by random forests. Chipman et al. (2010) show that, in terms of out of sample forecasting performance, BART is highly competitive with models such as random forests and produces more accurate forecasts in their experiments. Moreover, BART can be used for variable selection. In the context of the non-linear local projection, this feature provides information regarding the possible drivers of non-linearity.

The paper is organised as follows. Section 2 presents the empirical model. Section 3 reports the results from the simulation exercise. Section 4 shows the application to fiscal and financial shocks. Section 5 concludes.

2 Flexible local projections

In this section we outline the methodology, which we refer to as the BART-LP model, or flexible local projections. We discuss how BART-LP approximates the unknown conditional expectation function of local projection models, discuss the prior, and outline the posterior sampler. We then discuss how to compute generalized impulse responses to structural shocks within our framework.

2.1 The BART approximation

We work with the equation

$$y_{t+h} = m_h(\mathbf{z}_t, \mathbf{w}_{t+h}^{(h)}) + \epsilon_{t+h}^{(h)}, \quad (1)$$

where y_{t+h} denotes the scalar variable of interest, $h = 0, 1, \dots, H$ is the impulse response horizon, and $\epsilon_{t+h}^{(h)}$ satisfies $E(\epsilon_{t+h}^{(h)} | \mathbf{z}_t, \mathbf{w}_{t+h}^{(h)}) = 0$. We aim to study how y_{t+h} responds to a change in the scalar variable x_t , which is part of \mathbf{z}_t . The vector \mathbf{z}_t contains observable control variables, possibly including lagged values of y_t and contemporaneous and/or lagged values of other variables. The vector $\mathbf{w}_{t+h}^{(h)}$ contains additional control variables in the form of estimated residuals, as explained in Section 2.3. While \mathbf{z}_t is the same for every regression model h , $\mathbf{w}_{t+h}^{(h)}$ can potentially change. The function $m_h(\cdot)$ captures the true unknown conditional expectation function. The residual $\epsilon_{t+h}^{(h)}$ is assumed to be normally distributed with variance $\sigma_{t+h}^{2(h)}$. As noted in Jordà (2005), $\epsilon_{t+h}^{(h)}$ is serially correlated for $h \geq 1$.

It is common in the literature to assume a functional form for $m_h(\mathbf{z}_t, \mathbf{w}_{t+h}^{(h)})$. The most popular applications of LPs use a function of the type

$$y_{t+h} = g(q_t) \boldsymbol{\alpha}'^{(h)} \mathbf{z}_t + (1 - g(q_t)) \boldsymbol{\beta}'^{(h)} \mathbf{z}_t + \epsilon_{t+h}^{(h)}, \quad (2)$$

with q_t a transition variable capturing the nonlinearity of interest. The special case of

a linear model sets $g(q_t) = 1$, $\forall t$, and estimates the impulse response to a shock to x_t using the estimates for $\{\boldsymbol{\alpha}^{(h)}\}_{h=0}^H$ (Jordà, 2005). Non-linear applications typically specify a transition variable, assume a non-linear functional form for $g(\cdot)$, and compute non-linear impulse responses as a function of the estimates for $\{\boldsymbol{\alpha}^{(h)}, \boldsymbol{\beta}^{(h)}\}_{h=0}^H$. One advantage of this approach is that the specification of $g(q_t)$ and/or q_t makes it possible to form a clear economic interpretation of the non-linearity. One disadvantage is that it is hard for a single parametric model to study multiple types of non-linearities within the same framework.¹

Our paper differs from the existing literature by approximating the unknown conditional expectation function $m_h(\mathbf{z}_t, \mathbf{w}_{t+h}^{(h)})$ using Bayesian Additive Regression Trees (BART). It is assumed that

$$m_h(\mathbf{z}_t, \mathbf{w}_{t+h}^{(h)}) \approx f_h(\mathbf{z}_t, \mathbf{w}_{t+h}^{(h)} | \Gamma^{(h)}, \boldsymbol{\mu}^{(h)}) = \sum_{j=1}^J f_{h,j}(\mathbf{z}_t, \mathbf{w}_{t+h}^{(h)} | \Gamma_j^{(h)}, \boldsymbol{\mu}_j^{(h)}), \quad (3)$$

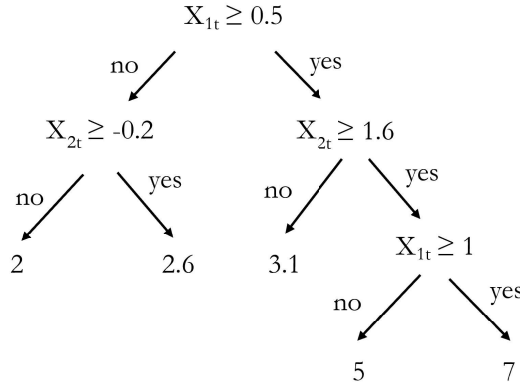
where $f_{h,j}(\mathbf{z}_t, \mathbf{w}_{t+h}^{(h)} | \Gamma_j^{(h)}, \boldsymbol{\mu}_j^{(h)})$ denotes a single regression tree j at horizon h and $f_h(\mathbf{z}_t, \mathbf{w}_{t+h}^{(h)} | \Gamma^{(h)}, \boldsymbol{\mu}^{(h)})$ denotes the sum of J regression trees. The parameters of the regression trees are the tree structures $\Gamma^{(h)} = [\Gamma_1^{(h)}, \dots, \Gamma_J^{(h)}]$ and the terminal nodes (or leaves) $\boldsymbol{\mu}^{(h)} = (\boldsymbol{\mu}_1^{(h)\prime}, \dots, \boldsymbol{\mu}_J^{(h)\prime})'$, with $\boldsymbol{\mu}_j^{(h)}$ of dimension $B_j \times 1$ and B_j the number of terminal nodes of tree j . Each regression tree divides the space of each explanatory variable by using binary splitting rules. Observations are assigned according to these splitting rules, and the terminal nodes return the fitted value conditional on the split. The fitted value of the dependent variable, based on a single regression tree, is then given by

$$f_{h,j}(\mathbf{z}_t, \mathbf{w}_{t+h}^{(h)} | \Gamma_j^{(h)}, \boldsymbol{\mu}_j^{(h)}) = \sum_{b=1}^{B_j} I(X_i) \mu_{j,b}^{(h)}, \quad (4)$$

¹For example, the smooth transition formulation by Auerbach and Gorodnichenko (2013a,b) sets $g(\cdot)$ equal to the logistic function, while the threshold formulation by Ramey and Zubairy (2018) and Alpanda et al. (2021) sets $g(\cdot)$ equal to the indicator function. This methodology is particularly suitable to study non-linearities over the state of the economy when the shock occurs, having specified q_t to capture how close the economy is to a recession or to an expansion.

where $I(\cdot)$ denotes an indicator function that equals 1 if X_i belongs to the set defined by the splitting rule implicit in $\Gamma_j^{(h)}$. Note that the complexity of each tree is determined by B_j , the number of terminal nodes. The functional form for f_h can potentially be very different across h , and the researcher does not need to introduce prior beliefs as to whether the tree structure differs considerably across horizons h .

Figure 1: Illustration of a tree (equation (5))



The following illustration helps set the ideas. Suppose that variable y_t is studied as a function of variables (x_{1t}, x_{2t}) using BART. Suppose, for simplicity, that only $J = 1$ tree is set by the researcher, and inference on the dataset $\{y_t, x_{1t}, x_{2t}\}_{t=1}^T$ has generated the following draw for the tree from the joint posterior distribution, also shown in Figure 1:

$$\begin{aligned}
y_t = & 2 \cdot I(x_{1t} < 0.5) \cdot I(x_{2t} < -0.2) + \\
& + 2.6 \cdot I(x_{1t} < 0.5) \cdot I(x_{2t} \geq -0.2) + \\
& + 3.1 \cdot I(x_{1t} \geq 0.5) \cdot I(x_{2t} < 1.6) + \\
& + 5 \cdot I(x_{1t} \geq 0.5) \cdot I(x_{2t} \geq 1.6) \cdot I(x_{1t} < 1) + \\
& + 7 \cdot I(x_{1t} \geq 0.5) \cdot I(x_{2t} \geq 1.6) \cdot I(x_{1t} \geq 1).
\end{aligned} \tag{5}$$

Suppose we aim to generate the expected value of y_t conditioning on some values $(\bar{x}_{1t}, \bar{x}_{2t})$. Then the expected value of y_t depends on which part of the regression

tree is reached by $(\bar{x}_{1t}, \bar{x}_{2t})$. For instance, (5) implies $E(y_t | \bar{x}_{1t} = 0, \bar{x}_{2t} = 1) = 2$ and $E(y_t | \bar{x}_{1t} = 0.8, \bar{x}_{2t} = 2) = 5$, as can be seen from the parts of the tree that are reached, given $(\bar{x}_{1t} = 0, \bar{x}_{2t} = 1)$ and $(\bar{x}_{1t} = 0.8, \bar{x}_{2t} = 2)$. A draw from the joint posterior distribution (which is informed by the data) must be viewed as a draw of the terminal nodes and of the structure of the tree leading to the nodes. In the notation used above, the draw of the terminal notes is $\boldsymbol{\mu} = (2, 2.6, 3.1, 5, 7)$, while the draw of the tree structure Γ consists of the selection of which variables are used for the splitting (in the illustration, both x_{1t} and x_{2t} are relevant for the splitting), the splitting values (0.5, -0.2, 1.6, 1), the number of terminal nodes ($B=5$), and how deep the tree goes (here, 2 layers). Other posterior draws from the joint posterior will generate alternative nodes and structures, hence alternative fitted values, even conditioning on the same covariates $(\bar{x}_{1t}, \bar{x}_{2t})$. If multiple trees are used, a sum of terminal nodes is used. Of course, the full structure of the algorithm generating the trees must be informed by the data, as also discussed below. BART can approximate potentially very nonlinear functions. We refer the reader to [Hill et al. \(2020\)](#) for a comprehensive review, and to [Section A](#) of the Online Appendix for a full illustration in a univariate model.

The model in equation (3) approximates $m_h(\mathbf{z}_t, \mathbf{w}_{t+h}^{(h)})$ using a sum of J trees. Each tree in the sum is restricted to be small *a priori* to avoid overfitting, and thus explains a small proportion of y_{t+h} (a ‘weak learner’). [Chipman et al. \(2010\)](#) show that a low value of J reduces predictive accuracy. As J increases, predictive performance initially improves, but this improvement tapers off, eventually. In practice, studies such as [Huber et al. \(2023\)](#) note that the difference in predictive accuracy is negligible for $J > 150$, and complex functions can be easily approximated using $J = 200$ or 250 . Caution should be given to attaching any structural interpretation to the trees. The tree structure is only used as a tool to explore the potentially nonlinear relationship among observables.

We stress that our paper takes BART as an off-the-shelf methodology, without contributing to its specification nor estimation. Rather, it explores its potential for

impulse response estimation. The use of BART to approximate the relationship between y_{t+h} and x_t has implications for the properties of the impulse responses. As the regression trees split the space of all covariates, the estimated predictions are dependent on the history of the covariates. Similarly, the shock to variable x_t can lead to predictions that differ in potentially very non-linear ways if the size and sign of the shock lead to the covariate space where the relationship between y_{t+h} and x_t is substantially different from the ‘average’ impact. This means that the same methodology can, in principle, capture multiple types of non-linearities within the same framework. Last, we stress that the methodology lends itself naturally to estimating impulse responses also using data from the Covid-19 period. Several parametric methods had to be adjusted to allow for the strong outliers associated with the pandemic, see for instance [Cascaldi-Garcia \(2022\)](#) and [Lenza and Primiceri \(2022\)](#). As discussed by [Clark et al. \(2023\)](#) in the context of a forecasting exercise, BART can accommodate large outliers by adjusting the estimated tree structure towards more extreme events. See also [Goulet Coulombe \(2024\)](#) and [Dinh et al. \(2024\)](#) for related methods for studying non-linearities in a non-parametric framework.

We now discuss estimation, and then return to a detailed discussion of non-linear impulse responses in the BART-LP model in [Section 2.4](#). [Section 3](#) then documents the performance of the methodology using Monte Carlo techniques.

2.2 Estimation

The model in equation (1) can be estimated using the MCMC algorithm described in [Chipman et al. \(2010\)](#), which we summarize here for completeness.

2.2.1 Priors

The prior distributions proposed by [Chipman et al. \(2010\)](#) play a crucial role, as they are devised to reduce the possibility of overfitting. The joint prior for the parameters

of the J trees of the model at each horizon h is factored as follows:

$$p((\Gamma_1^{(h)}, \boldsymbol{\mu}_1^{(h)}), (\Gamma_2^{(h)}, \boldsymbol{\mu}_2^{(h)}), \dots, (\Gamma_J^{(h)}, \boldsymbol{\mu}_J^{(h)})) = \prod_{j=1}^J p(\boldsymbol{\mu}_j^{(h)} | \Gamma_j^{(h)}) p(\Gamma_j^{(h)}), \quad (6)$$

where $p(\boldsymbol{\mu}_j^{(h)} | \Gamma_j^{(h)}) = \prod_{b=1}^{B_j} p(\mu_{b,j}^{(h)} | \Gamma_j^{(h)})$. The prior for the tree structure $\Gamma_j^{(h)}$ depends on the probability that the node at depth $d = 0, 1, 2, \dots$ is not a terminal node. This prior probability is given by $\alpha(1+d)^{-\beta}$ where $\alpha \in (0, 1)$ and $\beta > 0$. Higher values of β and smaller values of α reduce this probability and impose a stronger belief that the tree has a simple (i.e. shorter) structure. We follow the recommendation by Chipman et al. (2010) and set $\alpha = 0.95$ and $\beta = 2$. The prior for the threshold value c implies that this parameter is assumed to be uniform over the range of the values taken by the variables. In the default setting, the choice of splitting variables is also assumed to be uniform across the regressors.

To define $p(\boldsymbol{\mu}_j^{(h)} | \Gamma_j^{(h)})$ Chipman et al. (2010) first transform the dependent variable so that it lies between -0.5 and 0.5 . As a consequence, $m_h(\mathbf{z}_t, \mathbf{w}_{t+h}^{(h)})$ is also expected to lie between these values. The prior $p(\boldsymbol{\mu}_j^{(h)} | \Gamma_j^{(h)})$ is assumed to be normal $N(0, S)$. The variance S is set as $\frac{1}{2\kappa(J^{0.5})}$, with κ set to 2, the value recommended by Chipman et al. (2010). Under this default prior, there is a 95% probability that the conditional mean of the dependent variable lies between -0.5 and 0.5 .

A conjugate inverse χ^2 prior is used for the variance $\sigma_{t+h}^{2(h)}$. The hyperparameters of the prior distribution are set by using an estimate $\hat{\sigma}_{t+s}^{2(h)}$ of the variance obtained from a linear regression. If the true model is non-linear $\hat{\sigma}_{t+s}^{2(h)}$ will be biased upwards. Under the default prior, the hyperparameters are chosen so that $\Pr(\sigma_{t+s}^{(h)} < \hat{\sigma}_{t+s}^{(h)}) = 0.9$.

The total number of trees J is fixed.

2.2.2 MCMC algorithm

The MCMC algorithm devised by Chipman et al. (2010) samples from the conditional posterior distributions of $\sigma_{t+h}^{2(h)}$ and the parameters of the regression trees in each

iteration.² Each iteration of the algorithm samples from the following conditional posteriors:

1. conditioning on the tree structure, the error variance can be easily drawn from the inverse Gamma distribution;
2. the conditional posterior distribution of the tree structure is not known in closed form and a Metropolis-Hastings algorithm is used. Define $R_j^{(h)}$ as the residual:

$$R_j^{(h)} = y_{t+h} - \sum_{i \neq j} f(\mathbf{z}_t, \mathbf{w}_{t+h}^{(h)} | \Gamma_i^{(h)}, \boldsymbol{\mu}_i^{(h)}). \quad (7)$$

The j -th tree is proposed using the density $q(\Gamma_j^{new}, \Gamma_j^{old})$. Chipman et al. (2010) use a proposal density that incorporates 4 moves: (i) splitting the node into two new nodes (grow), (ii) transforming adjacent nodes to terminal node (prune), (iii) changing the decision rule of an interior node (change), (iv) swapping a decision rule between a node that is above and the node before it (swap). The probabilities associated with these moves are fixed at 0.25, 0.25, 0.4 and 0.1 respectively. The proposed tree structure Γ_j^{new} is accepted with probability

$$\alpha = \frac{q(\Gamma_j^{new}, \Gamma_j^{old}) p(R_j^{(h)} | \Gamma_j^{new}, \sigma_{t+h}^2) p(\Gamma_j^{new})}{q(\Gamma_j^{old}, \Gamma_j^{new}) p(R_j^{(h)} | \Gamma_j^{old}, \sigma_{t+h}^2) p(\Gamma_j^{old})}, \quad (8)$$

where $p(R_j | \Gamma_j, \sigma_{t+h}^2)$ is the conditional likelihood and $p(\Gamma_j)$ denotes the prior. This step is repeated for $j = 1, 2, \dots, J$ trees;

3. the conditional posterior distribution of the terminal node parameters is Gaussian with the parameters known in closed form. Therefore, the draw of $\boldsymbol{\mu}_j^{(h)}$ for $j = 1, 2, \dots, J$ can be carried out in a straightforward manner;
4. given a draw of the model parameters conditioning on $(\mathbf{z}_t, \mathbf{w}_{t+h}^{(h)})$, the predicted

²Intuitive descriptions of this MCMC algorithm can be found in Clark et al. (2023) and Hill et al. (2020).

value can be computed as

$$\sum_{j=1}^J f_{h,j}(\mathbf{z}_t, \mathbf{w}_{t+h}^{(h)} | \Gamma_j^{(h)}, \boldsymbol{\mu}_j^{(h)}) = \sum_{j=1}^J \sum_{b=1}^{B_j} I(\mathbf{z}_t, \mathbf{w}_{t+h}^{(h)}) \mu_{j,b}^{(h)}, \quad (9)$$

with $I(\mathbf{z}_t, \mathbf{w}_{t+h}^{(h)})$ an indicator function equal to 1 if $(\mathbf{z}_t, \mathbf{w}_{t+h}^{(h)})$ belongs to the splitting rule implied by $[\Gamma_1^{(h)}, \dots, \Gamma_J^{(h)}]$.

2.3 Autocorrelation

The residual term in LP models is known to be autocorrelated, a feature that must be taken into account in the estimation. In the case of linear local projections, it has been shown that the residual at horizon h follows a $MA(h - 1)$ process, see for instance Lusompa (2023). Lusompa (2023) suggests a GLS procedure whereby the autocorrelation is eliminated by including leads of the LP residuals from horizon $h = 0$ in the conditioning set.³

The non-parametric setting considered in this paper encompasses non-linear models. For the purpose of illustration, consider a simple non-parametric AR(1) model

$$y_{t+1} = v(y_t; A_1) + e_{t+1}. \quad (10)$$

Iterating the process forward 3 periods as an example gives

$$\begin{aligned} y_{t+2} &= v(v(y_t; A_1) + e_{t+1}; A_1) + e_{t+2}, \\ y_{t+3} &= v(v(v(y_t; A_1) + e_{t+1}; A_1) + e_{t+2}; A_1) + e_{t+3}. \end{aligned}$$

It is useful to compare this with a BART-LP for this horizon:

$$y_{t+3} = f_3(y_t | \Gamma_3, \boldsymbol{\mu}_3) + \epsilon_{t+3}^{(3)}. \quad (11)$$

³Lusompa (2023) suggests an efficient strategy that transforms the dependent variable of the LP regressions and does not require one to explicitly include the horizon 0 residuals as regressors.

The function $f_3(y_t|\Gamma_3, \boldsymbol{\mu}_3)$ approximates the non-linear relationship between y_t and its lead, but does not account for the dependence between the dependent variable and lagged shocks. Thus in this setting, the residual $\epsilon_{t+3}^{(3)}$ is a non-linear function of e_{t+1} and e_{t+2} , and has a non-linear autocorrelation structure.

In general, the Volterra expansion of any non-linear time-series shows its complex dependence on past shocks:

$$y_t = \sum_{i=0}^{\infty} \phi^i e_{t-i} + \sum_{i=0}^{\infty} \sum_{j=i}^{\infty} \zeta_{ij} e_{t-i} e_{t-j} + \sum_{i=0}^{\infty} \sum_{j=0}^{\infty} \sum_{k=0}^{\infty} \phi_{ij} e_{t-i} e_{t-j} e_{t-k} + \dots . \quad (12)$$

To account for this autocorrelation, we propose to include an estimate of the shocks,

$$\mathbf{w}_{t+h}^{(h)} = (\hat{e}_{t+1}, \hat{e}_{t+2}, \dots, \hat{e}_{t+h-1}), \quad (13)$$

as additional covariates in the h -period BART-LP. Following Lusompa (2023) we construct $\mathbf{w}_{t+h}^{(h)}$ at every horizon $h \geq 1$ using the residuals of the period $h = 0$ flexible local projection $y_t = f_0(\mathbf{z}_t, \mathbf{w}_t^{(0)} | \Gamma^{(0)}, \boldsymbol{\mu}^{(0)}) + \epsilon_t^{(0)}$, with $\mathbf{w}_t^{(0)} = \mathbf{0}$. Then, the flexible local projection for period h is specified as

$$y_{t+h} = f_h(\mathbf{z}_t, \mathbf{w}_{t+h}^{(h)} | \Gamma^{(h)}, \boldsymbol{\mu}^{(h)}) + \epsilon_{t+h}^{(h)}, \quad (14)$$

with $\mathbf{w}_{t+h}^{(h)}$ from equation (13). The BART approximation of the true non-linear function $m_h(\mathbf{z}_t, \hat{w}_{t+h}^{(h)})$ proxies the non-linear dependence of y_{t+h} on $e_{t+1}, e_{t+2}, \dots, e_{t+h-1}$ and ameliorates the autocorrelation in $\epsilon_{t+h}^{(h)}$.

It is important to note that alternative methods for dealing with autocorrelation in LPs have been proposed in the recent literature and these are also easily applicable in the proposed framework. For example, Montiel Olea and Plagborg-Møller (2021) show in the context of linear LPs that lag augmentation can preclude the need to use autocorrelation robust standard errors. In contrast, Ferreira et al. (2023b) modify the posterior distribution for the error variance in their Bayesian LP by using an

autocorrelation robust scale matrix. Contrary to these methods, we account for the autocorrelation structure of the error terms thanks to the inclusion of the estimated residuals $\mathbf{w}_{t+h}^{(h)}$. The Monte Carlo exercise from [Section 3](#) finds that omitting $\mathbf{w}_{t+h}^{(h)}$ from BART-LP leads to a loss in the efficiency of the estimator, see [Figure E.7](#) in the Online Appendix. [Section C](#) in the Online Appendix shows that error bands display reasonable coverage at short and medium horizons.

Frequency of components of covariates used in splitting rules can be used to judge the importance of variables in driving the non-linearity (see [Chipman et al., 2010](#) section 3.2). [Chipman et al. \(2010\)](#) recommend setting the number of trees to a small number for this exercise. This is to reduce the regularising influence of the prior and to encourage regressors to compete for inclusion as a splitting variable. Variable selection can be monitored by computing $v_i = \frac{1}{K} \sum_{k=1}^K z_{ik}$, where K denotes the number of MCMC iterations, i is the i -th regressor and z is the fraction of splitting rules that use this variable.

2.4 Generalized structural impulse responses

The computation of impulse responses to structural shocks relies on two conceptually different pillars: an identification scheme for the structural shock of interest, and a computational procedure to generate impulse responses. Our paper aims to advance the literature on the latter, without investigating the topic of identification in a non-parametric framework. We do acknowledge that identification is an important component of impulse response analysis, but stress that identification in a non-parametric framework goes beyond the scope of this paper, and mainly focus the analysis on impulse response computation.

Define \mathbf{y}_t a $k \times 1$ vector of random variables of interest at time t , with x_t potentially one of the entries of \mathbf{y}_t . Define ϕ_h the $k \times 1$ impulse response of \mathbf{y}_{t+h} to a structural shock to variable x equal to $\bar{\epsilon} h$ periods after the shock. Define y_{t+h} a generic entry of \mathbf{y} at period $t + h$, and ϕ_h the corresponding entry of ϕ_h . To simplify the illustration,

omit term $\mathbf{w}_{t+h}^{(h)}$ from equation (1) and specify BART-LP as

$$y_{t+h} = m_h(\mathbf{z}_t) + \epsilon_{t+h}^{(h)}. \quad (15)$$

Estimating impulse responses with model (15) requires two steps:

- a) specify \mathbf{z}_t and estimate (15) using the Bayesian procedure outlined in Section 2.2;
- b) use the estimated model to generate D independent predictions of y_{t+h} for $\mathbf{z}_t = \bar{\mathbf{z}}^0$ and $\mathbf{z}_t = \bar{\mathbf{z}}^1$, with $\bar{\mathbf{z}}^0$ capturing the covariates at the time when the shock occurs, and $\bar{\mathbf{z}}^1$ differing from $\bar{\mathbf{z}}^0$ by the shock $\bar{\epsilon}$. Compute generalized impulse responses as in Koop et al. (1996):

$$\phi_h = \frac{\sum_{d=1}^D m_h(\bar{\mathbf{z}}^1)}{D} - \frac{\sum_{d=1}^D m_h(\bar{\mathbf{z}}^0)}{D}. \quad (16)$$

Identification affects step a), in that different identification strategies imply different specifications of \mathbf{z}_t . By contrast, the actual type of non-linear impulse responses affects step b), in particular the definition of $\bar{\mathbf{z}}^0$. Possible non-linearities associated with the sign and size of the shock are modelled by appropriately selecting the sign and size of $\bar{\epsilon}$. (16) is similar, in spirit, to what Gonçalves et al. (2022) refer to as conditional average responses, as it averages out all other random terms in the model, and the shock of interest is not specified infinitesimally.

$\bar{\mathbf{z}}^0$ captures the values of the covariates when shock $\bar{\epsilon}$ hits the economy. As such, different candidate specifications for $\bar{\mathbf{z}}^0$ simulate different states of the economy at which the shock hits the economy. As an example, state contingent impulse responses that simulate a shock occurring in recessions will set $\bar{\mathbf{z}}^0$ to capture a prediction for y_{t+h} formed in a recessionary period. One way to do so is to select the periods in which the economy is in a recession, for instance based either on the NBER classification or on the value of real GDP growth relative to a threshold value, and then set $\bar{\mathbf{z}}^0$ equal to the sample average of \mathbf{z}_t restricted to such recessionary periods. To compute, instead,

a shock that occurs in normal economic times, one can set \bar{z}^0 equal to the average of z_t computed in the full sample. BART-LP allows for extensive flexibility over the specification of \bar{z}^0 , hence over the state of the economy when the shock occurs. Having set \bar{z}^0 , the calibration of the shock $\bar{\epsilon}$ captures the size of the shock. Non-linearities across the sign and size of the shock will be simulated by appropriately setting the value of $\bar{\epsilon}$.

It remains to identify the structural shocks of interest. Multiple options are available, which borrow from the existing literature on linear LP estimators. We refer the reader to [Section B](#) of the Online Appendix for a detailed discussion of how each approach can be coded within BART-LP. In short, BART-LP can be combined with three broad identification strategies, which all enjoy strengths and weaknesses. A first approach is to follow [Jordà \(2005\)](#) and rely on a separately estimated linear VAR model to identify the impact effect of the shocks of interest across a vector of variables. While this approach can conveniently exploit several identifications strategies already available for VAR models, it is subject to the important limitation that it imposes linearity in the impact effect of the shocks. Moreover, shock identification in a VAR model requires invertibility and as discussed in [Stock and Watson \(2018\)](#), the endogenous variables in the VAR should be chosen so that the reduced form residuals span the space of the structural shock(s) of interest (see also [Forni and Gambetti \(2014\)](#)). A second approach is to follow [Barnichon and Brownlees \(2019\)](#) and [Plagborg-Møller and Wolf \(2021\)](#) and replicate a recursive scheme within LP by using an appropriate set of control variables. This approach avoids using two-step procedures, yet it is more limited in the set of identifying restrictions used. A third approach is to use a proxy for the shock as a regressor or as an instrument for an endogenous covariate. One simple way to implement the latter approach is to assume a linear first stage and regress the endogenous regressor on the instrument and the set of controls z_t and include the fitted value as a regressor of interest in the main model. Note that this requires the instrument to be correlated with the shock of interest (relevance), to be

contemporaneously uncorrelated with other shocks (contemporaneous exogeneity) and to be uncorrelated with shocks at lags and leads (lag and lead exogeneity). As noted in [Stock and Watson \(2018\)](#), including appropriate controls in the LP is crucial in ensuring that this final condition is satisfied.⁴

3 Monte Carlo simulation

Since most of the existing parametric non-linear LP estimators can typically focus on only one non-linearity at a time, the specification of these models must be adapted each time in light of the specific non-linearity considered (see, for instance, the discussion in [Barnichon, Debortoli and Matthes, 2022](#)). We use Monte Carlo simulations to show that the same BART-LP methodology can, instead, recover the true non-linear patterns of very different non-linear models. We use three different data generating processes to study three different types of non-linearities: over the size of the shock, the sign of the shock, or the timing at which the shock occurs. Simulation results suggest that the same BART-LP can recover the true impulse responses irrespectively of the underlying non-linearity of the model. We also show that BART-LP performs well when the data generating process is linear.

In all simulations, we generate $T = 300$ observations, discard the first 100 observations and use the remaining 200 observations for estimation, as in [Jordà \(2005\)](#). BART-LP is estimated using $J = 250$ trees, adding the estimated fitted residuals to control for autocorrelation and generating 2,000 posterior draws. Each simulation is repeated 500 times. Unreported analysis confirms that the results further improve when the sample size increases to $T = 500$, as expected. [Figure E.7](#) in the Online Appendix documents the loss of efficiency in the estimation of the impulse responses when omitting the residual $\mathbf{w}_{t+h}^{(h)}$ from BART-LP for all the simulated models considered,

⁴Note, however, that the conditions in [Stock and Watson \(2018\)](#) pertain to a *linear* LP and it is likely that the non-parametric nature of the proposed model requires more stringent conditions. For example, if the dependent variable in the LP is a non-linear function of past shocks, then this dependence should be accounted for by including appropriate control variables.

see the discussion in [Section 2.3](#).

Impulse response estimation via local projections can be subject to large variances ([Li et al., 2024](#)) and finite sample biases ([Herbst and Johannsen, 2024](#)). The simulations in this section and the analysis in [Section C](#) in the Online Appendix both suggest that the variance from the estimation of BART-LP is not quantitatively large. [Figure E.4-Figure E.5-Figure E.6](#) in the Online Appendix confirm that the results of the analysis hold also for $T = 100$, suggesting that finite sample issues do not necessarily invalidate the methodology. See also [Ho et al. \(2024\)](#) for an alternative and very general approach that estimates impulse responses via prediction pools across multiple models.

3.1 SVAR-GARCH model: size of the shock

The first model we use for simulations is the model from Section III.B in [Jordà \(2005\)](#),

$$\begin{pmatrix} y_{1t} \\ y_{2t} \\ y_{3t} \end{pmatrix} = A \begin{pmatrix} y_{1t-1} \\ y_{2t-1} \\ y_{3t-1} \end{pmatrix} + Bh_t + \begin{pmatrix} \sqrt{h_t}\epsilon_{1t} \\ \epsilon_{2t} \\ \epsilon_{3t} \end{pmatrix}, \quad (17)$$

$$(\epsilon_{1t}, \epsilon_{2t}, \epsilon_{3t})' = \boldsymbol{\epsilon}_t \sim N(\mathbf{0}, I_3), \quad (18)$$

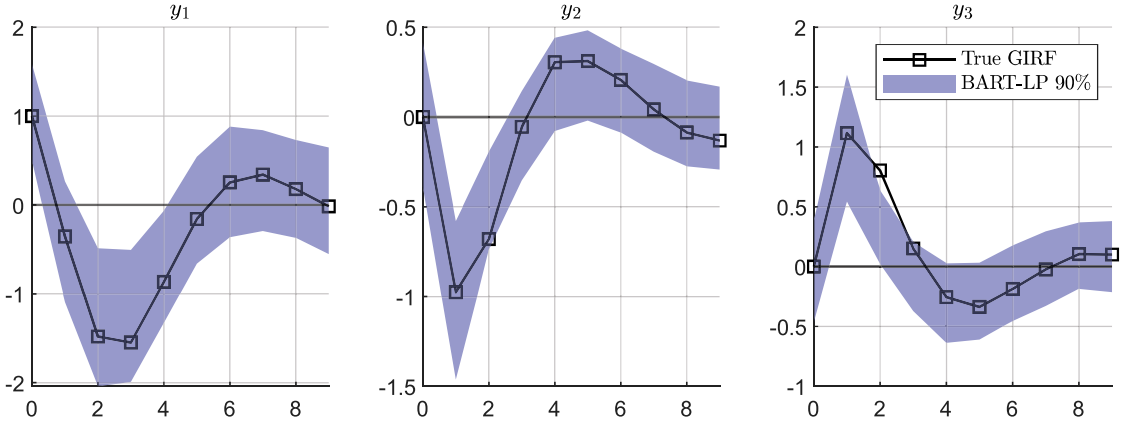
$$h_t = 0.5 + 0.5h_{t-1} + 0.3\sqrt{h_{t-1}}\epsilon_{1t-1}, \quad (19)$$

$$B = \begin{pmatrix} -1.75 \\ -1.5 \\ 1.75 \end{pmatrix} \quad A = \begin{pmatrix} 0.5 & -0.25 & 0.25 \\ 0.75 & 0.25 & 0.25 \\ -0.25 & -0.25 & 0.75 \end{pmatrix}. \quad (20)$$

In this model, each shock i affects only variable i contemporaneously, while all shocks affect all variables after one period. Contrary to the second and the third shock, the first shock features time-varying variance, and the size of the shock matters non-

linearly for its propagation through the system.⁵

Figure 2: SVAR-GARCH - true and estimated impulse responses



We use a simulation exercise to study how well the BART-LP methodology recovers the true impulse responses associated with a shock to y_{1t} of size 1. We first use generalized impulse responses to simulate the true impulse responses associated with $\epsilon_{1t} = 1$. Then, on each generated dataset, we estimate BART-LP by setting the first entry of \mathbf{z}_t equal to the contemporaneous realization of the first shock and two lags of all three variables. We compute the median generalized impulse responses by simulating a shock $\bar{\epsilon} = 1$, setting $\bar{\mathbf{z}}^0$ equal to the sample average for each horizon h . We replicate the analysis 500 times and store the pointwise median responses estimated using BART-LP.

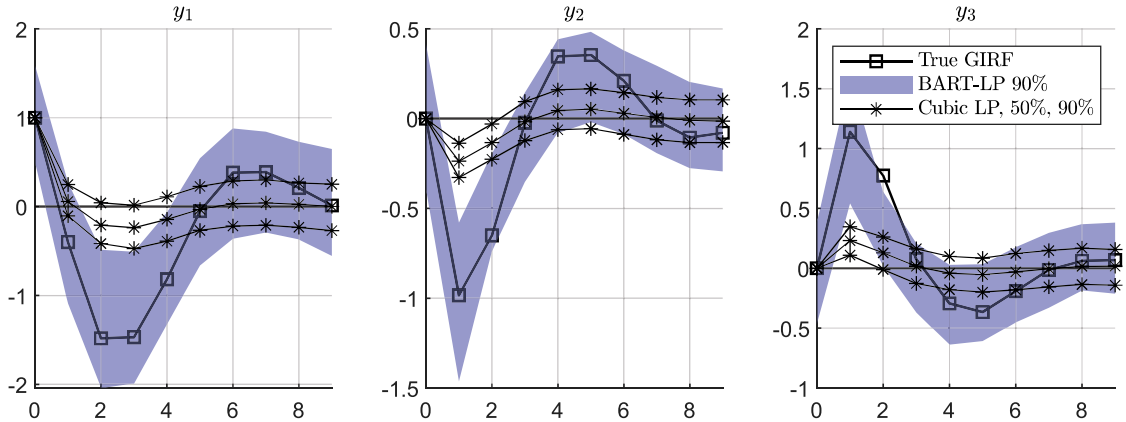
Figure 2 reports the results of the analysis. The squared black line shows the true generalized impulse responses. The shock increases y_{1t} on impact by 1 and generates no contemporaneous response in (y_{2t}, y_{3t}) . It subsequently generates an oscillating pattern in all variables. The continuous line and the shaded area report the pointwise median and 90% band computed over the median response across the 500 simulations. The first result documented in Figure 2 is that BART-LP correctly detects that only

⁵We code the simulation exercise following the exact code available in the replication files from Jordà (2005).

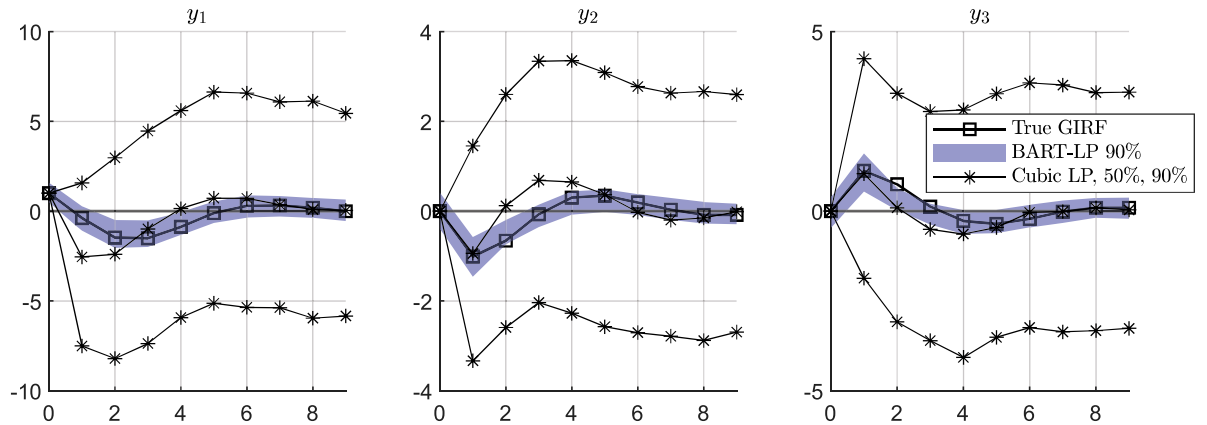
y_1 contemporaneously responds to ϵ_1 . This result is not imposed by the BART-LP methodology, contrary to a linear recursive VAR model or to linear LP estimators where the shock is identified using controlled variables (Barnichon and Brownlees, 2019). BART-LP correctly detects that (y_2, y_3) take at least one period to respond to the shock, as indicated by the 90% band for these variables containing zero on impact. The second result documented in Figure 2 is that BART-LP captures well the full dynamic evolution of all variables at several horizons of interest. BART-LP detects the oscillating pattern of all variables, including the zero long run effect of the shock on all variables.

Figure 3: SVAR-GARCH - comparison to parametric cubic LP

A) Cubic evaluated at the mean



B) Cubic evaluated above the mean



We compare how BART-LP performs relative to parametric non-linear LP estimators. It is not immediately clear which option is best suited for this comparison given the specific data generating process at hand. We use the cubic local projection by Jordà (2005) because it is one of the few existing parametric non-linear LP specifications that can jointly address multiple non-linearities (over size, sign and history), a feature which we argued is also a convenient feature of BART-LP. On each replication we estimate the cubic LP as in Jordà (2005). We then compute two impulse responses, which differ depending on the history at which the responses is evaluated: at the mean of the data (discussed but not reported by Jordà, 2005) or at five standard deviations from the mean (reported by Jordà, 2005 in his Figure 3). We report the median and the 90% band of the OLS estimator over 1,000 replications.

The comparison is shown in Figure 3. As discussed by Jordà (2005), evaluating the cubic LP at the mean of the data captures the correct shape of the true impulse responses, yet it quantitatively underestimates the overall effect. By contrast, evaluating the cubic LP away from the mean does a better job only when focusing on the median effect, while implying a higher variance. It follows that the cubic LP estimator requires careful selection of the initial conditions and potentially leads to high variance. By contrast, BART-LP works well both on the mean and the variance. In the rest of the Monte Carlo exercise we omit further comparisons to parametric non-linear LP estimators. The aim of the exercise is not to inspect if BART-LP can recover the data generating process more successfully than any parametric non-linear LP. The aim it to show that BART-LP does not require adjusting to a specific non-linearity, in that the same method can address very different types of non-linearities. By contrast, parametric non-linear methods need to be fine tuned to capture one non-linearity or the other.

3.2 Nonlinear Moving Average model: sign of the shock

The second model we use for simulation is

$$\mathbf{y}_t = \sum_{l=0}^{20} \boldsymbol{\beta}_{gdp,l} \cdot \epsilon_{gdp,t-l} + \sum_{l=0}^{20} \boldsymbol{\beta}_{\pi,l} \cdot \epsilon_{\pi,t-l} + \quad (21)$$

$$+ \sum_{l=0}^{20} \left[\boldsymbol{\beta}_{ff,l}^+ \cdot I(\epsilon_{ff,t-l} \geq 0) + \boldsymbol{\beta}_{ff,l}^- \cdot I(\epsilon_{ff,t-l} < 0) \right] \cdot \epsilon_{ff,t-l}, \quad (22)$$

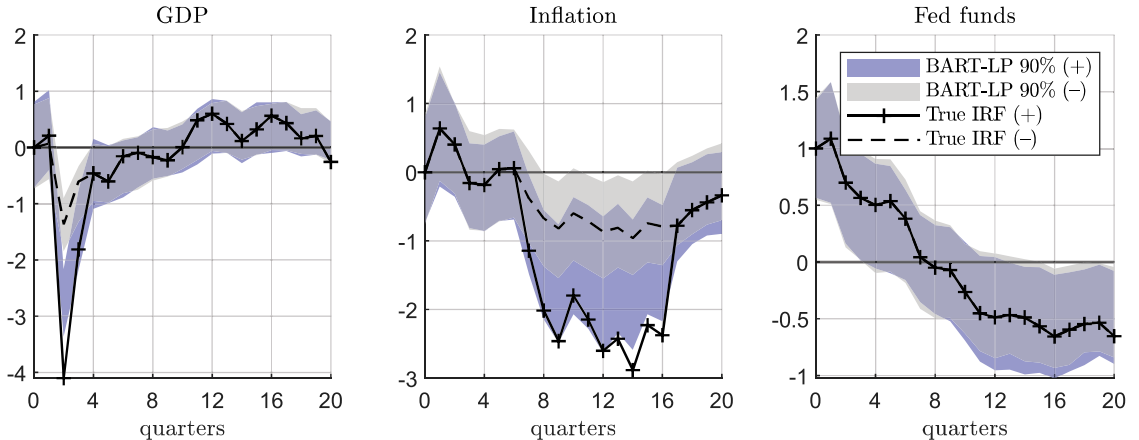
$$\epsilon_t \sim N(\mathbf{0}, I), \quad (23)$$

with $\mathbf{y}_t = (gdp_t, \pi_t, ff_t)'$ a vector containing real GDP, inflation, and the federal funds rate, and $\boldsymbol{\epsilon} = (\epsilon_{gdp,t}, \epsilon_{\pi,t}, \epsilon_{ff,t})'$ a vector of structural shocks. The model is a moving average process of order 20 driven by three structural shocks: a GDP shock, an inflation shock, and a monetary policy shock. The monetary policy shock affects the variables differently at each horizon $t+h$ depending on whether the monetary policy shock at time t is positive or negative. The true impulse responses are captured by $\{\boldsymbol{\beta}_{gdp,l}\}_{l=0}^{20}$ for the GDP shock, by $\{\boldsymbol{\beta}_{\pi,l}\}_{l=0}^{20}$ for the inflation shock, and by $\{\boldsymbol{\beta}_{ff,l}^+, \boldsymbol{\beta}_{ff,l}^-\}_{l=0}^{20}$ for the positive and negative monetary policy shock.

We calibrate the model following an approach similar to [Barnichon and Brownlees \(2019\)](#). We first estimate a recursive VAR model on US real GDP, inflation and the federal funds rate to estimate linear impulse responses to a GDP shock, an inflation shock and a monetary policy shock. We then set $\{\boldsymbol{\beta}_{gdp,l}, \boldsymbol{\beta}_{\pi,l}, \boldsymbol{\beta}_{ff,l}^+, \boldsymbol{\beta}_{ff,l}^-\}_{l=0}^{20}$ equal to the estimated impulse responses to three shock: the GDP shock, the inflation shock, and the monetary policy shock. Last, we set $\boldsymbol{\beta}_{ff,l}^+ = \boldsymbol{\beta}_{ff,l}^-$ for every l , with two exceptions: (1) at horizons $l = 2, 3$ the first entry of $\boldsymbol{\beta}_{ff,l}^+$ equals 3 times the first entry $\boldsymbol{\beta}_{ff,l}^-$, and (2) at horizons $l = 7, 8, \dots, 16$ the second entry of $\boldsymbol{\beta}_{ff,l}^+$ equal 3 times the second entry of $\boldsymbol{\beta}_{ff,l}^-$. This implies a data generating process in which positive monetary policy shocks affect output and inflation 3 times more than negative shocks in the short term (for output) and in the medium term (for inflation) horizons.

We design the simulation exercise as follows. On each generated dataset, we esti-

Figure 4: Sign-dependent Moving Average - true and estimated impulse responses

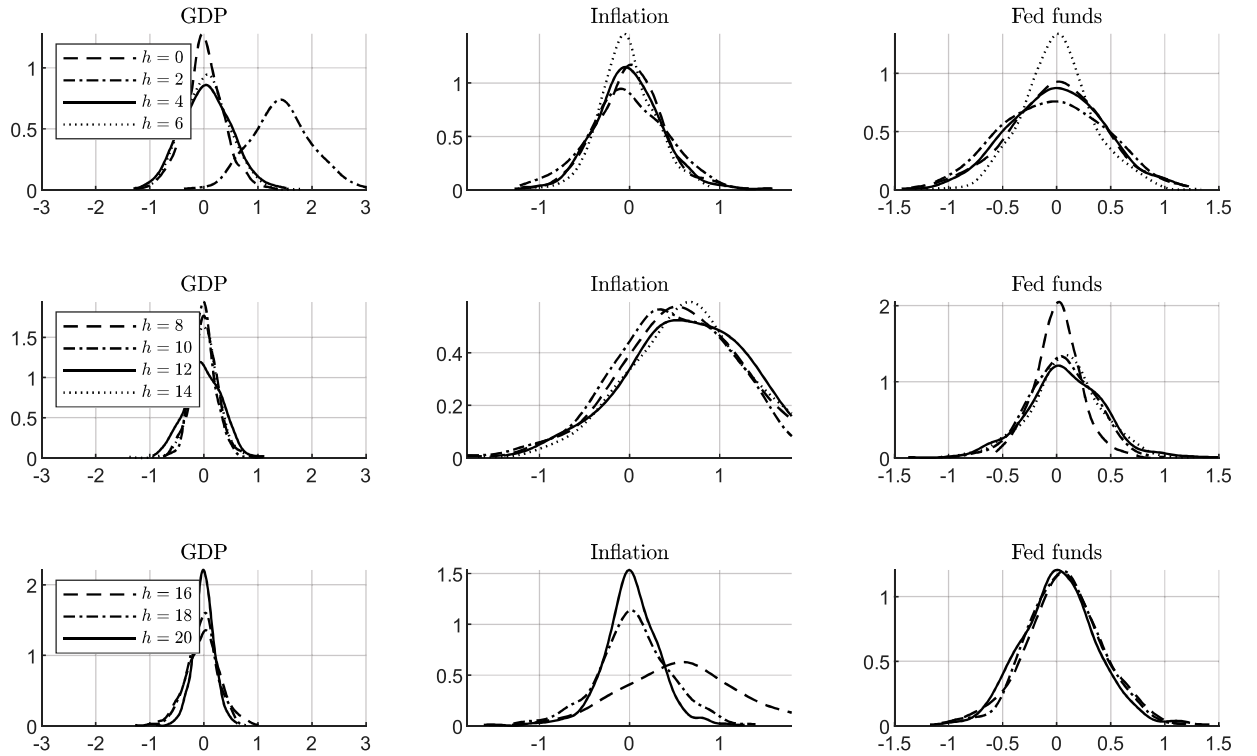


Note: The response to a negative shock has been flipped in sign to improve comparison.

mate the BART-LP model by setting the first entry of \mathbf{z}_t equal to the contemporaneous realizations of the monetary shocks and two lags of all three variables. We compute numerically the median generalized impulse responses by simulating a shock of size $\bar{\epsilon} = +1$ or $\bar{\epsilon} = -1$, setting $\bar{\mathbf{z}}^0$ equal to the sample average for each horizon h . Last, we replicate the analysis 500 times and store the pointwise median responses from BART-LP.

Figure 4 shows the impulse responses. The (+) and (−) lines show the true impulse responses associated with a positive and a negative monetary policy shock, respectively. The responses to a negative shock are reported with flipped sign to improve the comparison. By construction, the true response of the federal funds rate does not change in the sign of the shock, while the true response of GDP and inflation is 3 times stronger in response to a positive shock in selected periods. The blue and grey shaded areas report the 90% pointwise posterior bands associated with the BART-LP model following a positive and a negative shock, respectively. BART-LP correctly detects several features of the data generating process. First, that the impact effect of the monetary shock on GDP and inflation is zero, a feature that is not introduced as an

Figure 5: Sign-dependent Moving Average - difference in the positive and negative response to a monetary policy shock



identifying restrictions, but that is found by estimation. Second, that the response of the federal funds rate is symmetric, as shown by the 90% bands in response to a positive and a negative shock being effectively identical (up to the sign), a feature not introduced by construction in our methodology. Third, that GDP and inflation respond more strongly to a positive than to a negative shocks in selected horizons, and largely symmetrically in other horizons. The negative response is estimated correctly qualitatively and quantitatively, with the true impulse response sitting approximately in the middle of the bands. The estimated positive response is qualitatively correct although it somewhat underestimates the true response, especially for inflation.

Figure 4 only reports the pointwise marginal distributions, hence it cannot fully

display the strength of the asymmetry in the response to positive and negative shock. Figure E.5 complements the analysis by reporting, for different horizons h , the distribution of the difference in the absolute values of the responses to a positive and negative shocks. Under symmetry, this difference should be centred at 0. The figure shows that the distribution for the federal funds rate are always centred at 0 for all horizons, consistent with the data generating process. In the short horizon, BART-LP correctly detects that GDP responds more to a positive than to a negative shock. For horizons 2 and 3 it attaches as much as 88% and 95% posterior probability to the event that the response to a positive shock is stronger than to a negative shock, in absolute value. This event is indeed true in the data generating process. Last, BART-LP also correctly detects that inflation responds more strongly to positive shocks than to negative shocks at horizons 7 to 16. The posterior probability attached to the difference in the impulse responses being positive is between 75% and 85%, depending on the exact horizon considered. Last, the posterior probability mass is equally split between a stronger and a weaker response to a positive relative to a negative shocks for the horizons in which the data generating process is indeed symmetric.

3.3 Threshold VAR model: timing of the shock

The third model we use for simulations is

$$\mathbf{y}_t = [\Pi_1 \mathbf{y}_{t-1} + B_1 \boldsymbol{\epsilon}_t] \cdot \mathbb{I}(y_{3,t-1} \leq 0) + [\Pi_2 \mathbf{y}_{t-1} + B_2 \boldsymbol{\epsilon}_t] \cdot \mathbb{I}(y_{3,t-1} > 0), \quad (24a)$$

$$\boldsymbol{\epsilon}_t \sim N(\mathbf{0}, I), \quad (24b)$$

with $\mathbf{y}_t = (y_{1t}, y_{2t}, y_{3t})'$, $\boldsymbol{\epsilon}_t = (\epsilon_{1t}, \epsilon_{2t}, \epsilon_{3t})'$ and

$$\Pi_1 = \begin{pmatrix} 0.25 & -0.25 & 0.25 \\ 0.25 & 0.25 & 0.25 \\ -0.25 & -0.25 & 0.15 \end{pmatrix}, \quad B_1 = \begin{pmatrix} 0.10 & 0 & 0 \\ -0.20 & 0.15 & 0 \\ 0.10 & -0.10 & 1 \end{pmatrix}, \quad (25)$$

$$\Pi_2 = \begin{pmatrix} 0.50 & -0.25 & 0.25 \\ 1.25 & 0.50 & 0.25 \\ -1.75 & -1.25 & 0.15 \end{pmatrix}, \quad B_2 = \begin{pmatrix} 0.10 & 0 & 0 \\ -0.20 & 0.15 & 0 \\ 0.10 & -0.10 & 0.40 \end{pmatrix}. \quad (26)$$

The model is a recursive Threshold Vector Autoregressive model that jumps across two regimes depending on the evolution of the third variable. See, for instance, [Castelnovo and Pellegrino \(2018\)](#). Note that the non-linear evolution of the system is endogenous rather than exogenous, making inference potentially more challenging ([Gonçalves et al., 2022](#)).

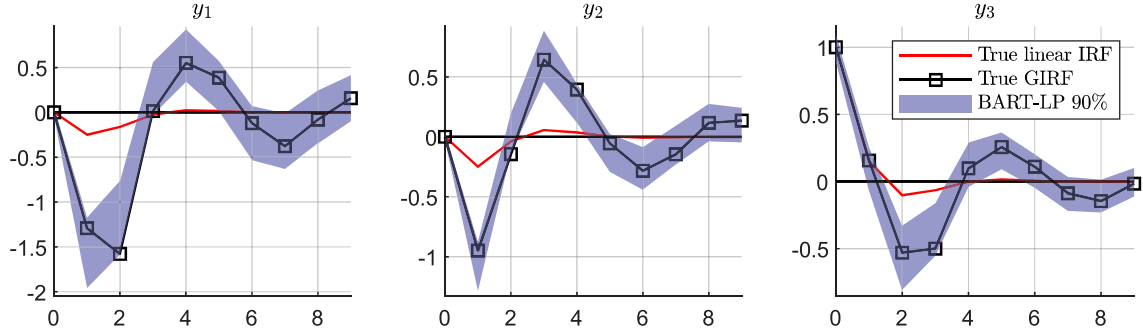
We first compute the true generalized impulse responses to a positive one-standard-deviation shock to y_{3t} in regime 1 by setting the initial condition of the impulse response to $\mathbf{y}_0 = \mathbf{0}$ and generalizing over contemporaneous and future structural shocks. We then study how well the BART-LP estimator recovers the true impulse responses. On each generated dataset, we estimate the BART-LP model by setting \mathbf{z}_t equal to all three contemporaneous variables as well as two lags of the variables.⁶ We hence identify the model by controlling for contemporaneous variables to achieve recursive identification. We then compute the median generalized impulse response by simulating a shock $\bar{c} = +1$, setting $\bar{\mathbf{z}}^0$ equal to the sample average for each horizon h , except that the entry for y_{3t} is set to 0. Last, we replicate the analysis 500 times and store the pointwise median responses for the BART-LPs.

The top panel of [Figure 6](#) shows the results of the exercise. The shock hits the system when the system is in regime 1. Under linearity, the model would stay in

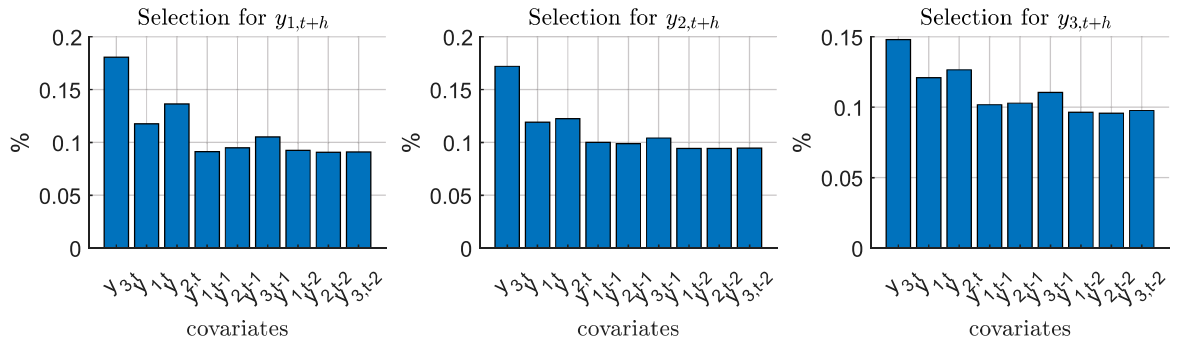
⁶We use two lags of the variables for comparability with the Monte Carlo exercises run so far. The results remain unchanged when using one lag, as suggested by the data generating process.

Figure 6: Threshold VAR model

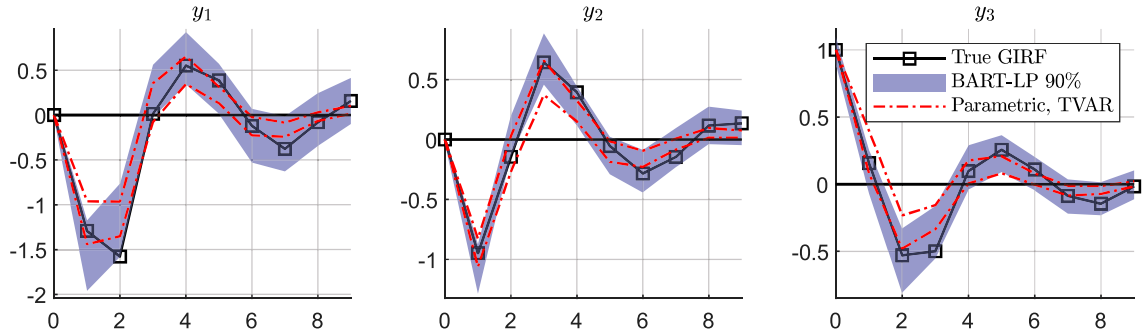
A) True and estimated impulse responses



B) Splitting variables from BART



C) Compare to parametric TVAR estimates



Note: Caution should be paid in attaching a structural or economic interpretation to the selection of variables used by BART as splitting variables. The results on how frequently the estimated residuals $\mathbf{w}_{t+h}^{(h)}$ featured as splitting variables were omitted to improve visibility.

regime 1, with an impulse response uniquely pinned down by (Π_1, B_1) and shown by the continuous red line. Instead, the non-linearity of the model implies an endogenous evolution across regimes, in accordance with the endogenous response of y_{3t} . The squared black line represents the true generalized impulse responses. The two lines differ. The impulse response estimated via BART-LP correctly estimates the true generalized impulse response. First, the model captures very well the zero impact effect of the shock on y_1, y_2 , even though the methodology does not impose this feature. Second, the model correctly captures the dynamic evolution of all three variables. It detects that the endogenous evolution across regimes makes the response of the first two variables more pronounced compared to a linear model that remains in regime 1.

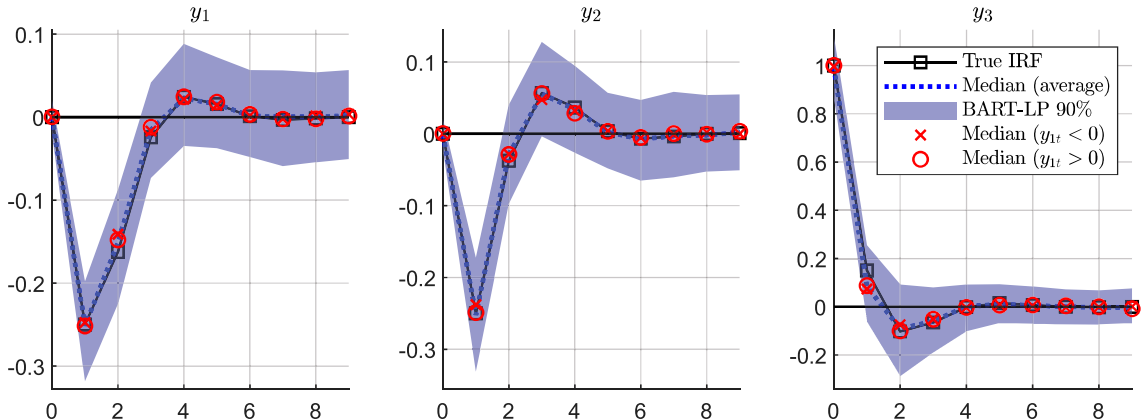
As we argued in [Section 2.3](#), an additional convenient feature of BART-LP is that it estimates how frequently each regressor is used as a splitting variable in the tree structure from the posterior distribution. Contrary to the models considered so far, the TVAR model lends itself particularly well for this analysis, because we know that y_{3t} should play a prominent role in the splitting of the covariate parameter space. The middle panel of [Figure 6](#) shows the results from the simulation exercise. For each variable, it shows how frequently each covariate was used as a splitting variable, computed across all covariates and across all replications. BART indeed correctly detects that $y_{3,t}$ is more relevant as a splitting variable compared to any other covariates, which is in line with the data generating process. The lower panel of [Figure 6](#) complements the analysis by reporting the impulse responses estimated from the parametric Threshold VAR model by [Alessandri and Mumtaz \(2017\)](#). While assuming knowledge of the true parametric form of the model does deliver tighter posterior impulse responses, we find that BART performs very well without needing to assume a functional form for the data generating process.

3.4 Linear VAR model

We conclude the simulation exercise by documenting how BART-LP performs when the data generating process is linear. We start from the threshold VAR model from (24). We then set $\Pi_2 = \Pi_1$ and $B_2 = B_1$, reducing a model to a linear VAR model of order 1. We then study the response to the third shock of the model, as in Section 3.3.

We design the simulation exercises as in Section 3.3. We first compute the true linear impulse response to a positive one-standard deviation shock to y_{3t} . Then, on each generated dataset, we estimate BART-LP by setting z_t equal to all three contemporaneous variables as well as two lags of the variables. We use this procedure to identify the last shocks of the model recursively. We store the median generalized impulse response over 500 replications.

Figure 7: Linear VAR model



The results of the analysis are shown in Figure 7. The shaded blue area is computed as in the previous figures and reports the pointwise 68% bands across median impulse responses. The bands show that BART-LP captures the true linear impulse responses perfectly well. This holds true both on impact and at every future horizon. We then explore if BART-LP successfully detects that the impulse responses of this data generating process do not change depending on the initial condition that hold at the time at which the shock hits the system. The blue dashed line shows the pointwise median value associated with the blue bands, where the generated impulse are

computed conditioning on the average sample value of the covariates. The starred and circled red lines show the median impulse responses when replicating the analysis by simulating impulse responses setting the initial condition to randomly extracted periods in which the first variable was positive or negative, respectively. Since the data generating process is linear, the true impulse responses do not depend on the initial condition in which the shock hits the system. The BART-LP methodology successfully detects that the impulse responses are linear and independent from the initial condition. All in all, BART-LP proves to perform successfully both in variety of non-linear worlds and in a linear environment.

4 Empirical analysis

In this section, we apply the proposed model to two recent issues that have featured prominently in the empirical literature on non-linear macroeconomic dynamics, one on financial shocks, the other on monetary shocks.

4.1 The non-linear effects of financial shocks

Several contributions in the economic literature have studied if financial market disruptions can have strong effects on the real economy. While previous research has addressed this question using linear models, [Barnichon, Matthes and Ziegenbein \(2022\)](#) document that the effects of financial shocks are stronger in response to adverse shocks compared to favourable shocks. This result helped reconcile existing empirical findings from linear models, which drew contradicting conclusions as to whether financial shocks can or cannot generate long and deep economic recessions ([Romer and Romer, 2017](#) and [Gilchrist and Zakrajšek, 2012](#), respectively). [Forni et al. \(2024\)](#) reconsider the results by [Barnichon, Matthes and Ziegenbein \(2022\)](#) by studying two non-linearities within the same framework, and find that the results by [Barnichon, Matthes and Ziegenbein \(2022\)](#) mainly hold in response to large shocks, but not to small shocks.

The model used by Barnichon, Matthes and Ziegenbein (2022) and Forni et al. (2024) are parametric, and only use pre-Covid data. We use our BART-LP methodology to reassess their results in a non-parametric framework, and study if the results are sensitive to using the Covid period in the analysis. In particular, we use BART-LP to assess how the joint non-linearities documented by Forni et al. (2024) change if one does not introduce their cubic functional constraint on how the two non-linearities interact. We set y_{t+h} from equation (1) equal to six possible variables: (1) the annual growth of industrial production, (2) the annual growth of CPI inflation, (3) the unemployment rate, (4) the excess bond premium by Gilchrist and Zakrajšek (2012), (5) the stock returns, and (6) the federal funds rate. The results are insensitive to monotone transformations of the data, see Chipman et al. (2010). The data is monthly and runs from 1973M1 to either 2020M2 or 2024M12, depending on whether the Covid pandemic is included. We add 6 lags of all variables.⁷

Since our contribution is closely related to Forni et al. (2024), we ensure comparability by using their same identification strategy, which, in turn, builds on Gilchrist and Zakrajšek (2012). We identify the financial shock as the shock that affects fast moving variables, but not slow moving variables. We estimate a preliminary linear SVAR model using the above ordering of the variables and estimate the impact vector associated with the entry of the excess bond premium in a recursive identification. A shortcoming of this approach is that it relies on a parametric model to study the impact effects of the shocks, exploiting the non-parametric part of the model only from the second month from the shock. In addition to improving comparability with Forni et al. (2024), this modelling strategy has the advantage that it allows calibrating the financial shock to generate an impact effect of the excess bond premium of an intended size. This allows inspecting how the results progressively change when the shock is marginally increased to generate impact variations in the excess bond premium be-

⁷The excess bond premium is downloaded from the federal reserve [website](#). Stock returns are calculated using the Standards and Poor total return index obtained from Global Financial database. The remaining variables are taken from the FRED database.

tween 50 and 300 basis points.⁸ We simulate positive and negative shocks, considering either a shock $\bar{\epsilon}$ that moves the excess bond premium by ± 50 basis points or by ± 300 basis points. We set \bar{z}^0 equal to the sample average of z_t . We set the number of trees to 500 and use 4,000 posterior draws, with a burn-in of 2,000 draws. The code takes approximately one hour to run.

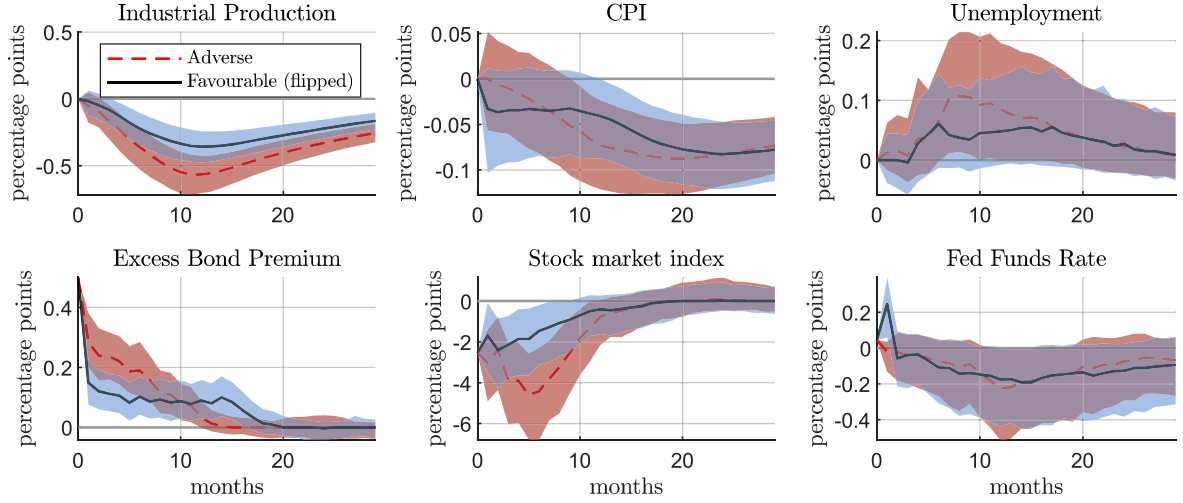
The results of the analysis are shown in Figure 8-Figure 9, which report the impulse responses associated with the small (Figure 8) and the large (Figure 9) exogenous variation of the excess bond premium. The figures report the results using both the sample until before Covid (top panels) or the full sample (bottom panel). All panels report the response to an adverse shock and to a favourable shock, interpreted as shocks that increase or decrease the excess bond premium, respectively. The response to favourable shocks has been multiplied by -1, to improve the comparison. The response of industrial production and CPI is shown as the cumulated average response. The figure reports the pointwise median response together with the 90% posterior coverage bands.

Figure 9 shows that when the magnitude of the financial shock is relatively small, systematic evidence for differences in responses across the sign of the shock is largely absent irrespectively of the sample size used for the analysis. The timing and scale of the response of industrial production to a favourable shock is largely the mirror image of the response to an adverse shock. The stock market response is stronger and more long-lasting in response to an adverse shock, a result consistent with the more persistent response of the excess bond premium. Yet, this asymmetry does not result into an asymmetric response of the real economy. The results hold under both samples: the only detectable difference when also using post-Covid data is that

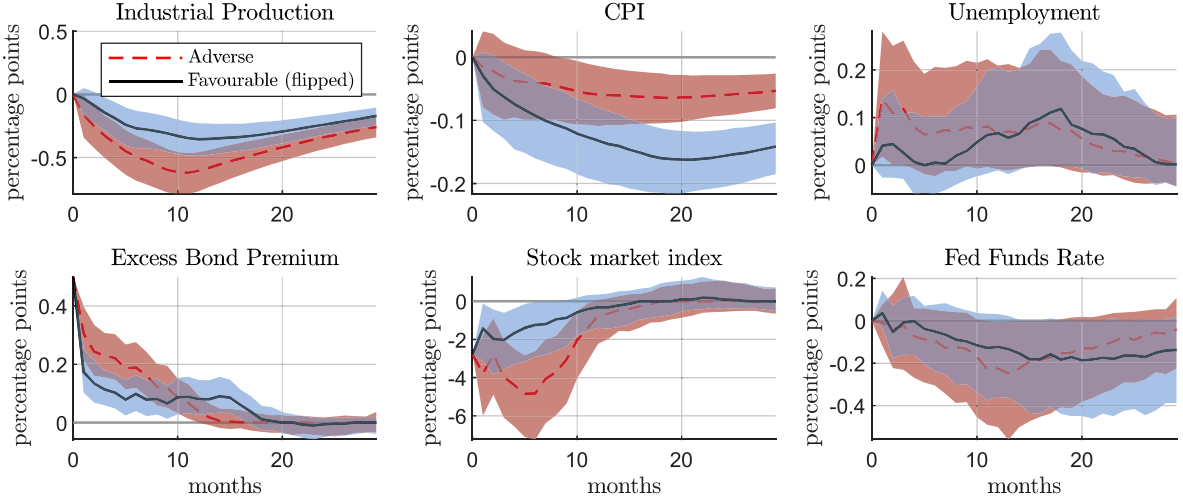
⁸While the linear VAR identification approach used in this application has its merits, it implies that any non-linear impact effect of the shocks associated with the (unknown) data generating process generates model misspecification. We conjecture that the implication would be to estimate an average impact effect of the shocks that weights the true non-linear impact effects. We caution against this limitation of the methodology. We stress that the paper does not aim to advance the literature on shock identification in a non-parametric framework, a task which is beyond the scope of this paper.

Figure 8: Nonlinear effects of financial shocks - Small shock, adverse versus favourable

A) Pre-Covid sample, 1973M1-2020M2



B) Post-Covid sample, 1973M1-2024M12

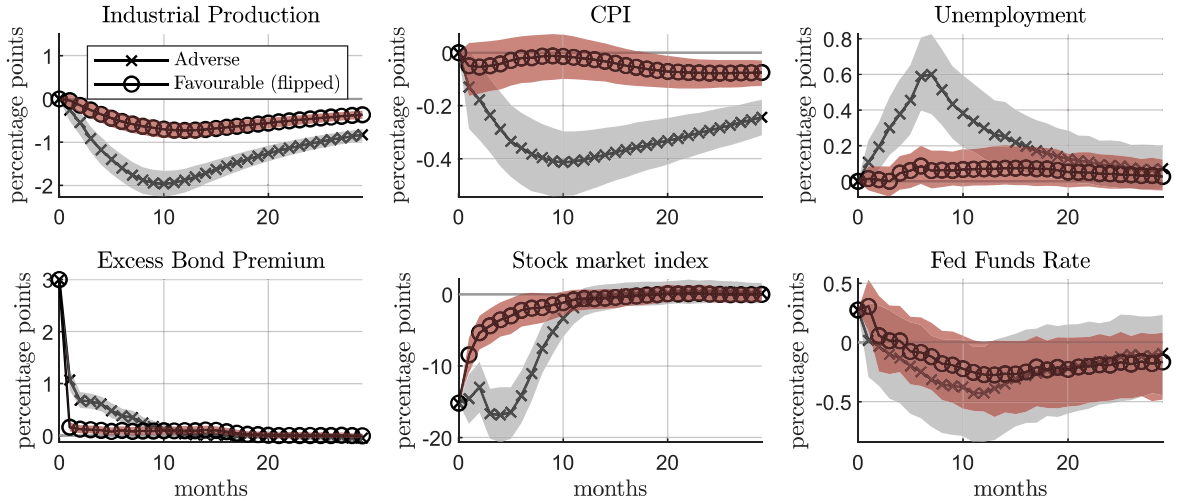


Note: Response to adverse and favourable financial shocks that change the excess bond premium by 50 basis points (top panel) or 300 basis points (bottom panel). The response to favourable shocks has been multiplied by -1 for the purpose of comparison. The lines and bands reported are the pointwise median and 90% coverage bands, respectively.

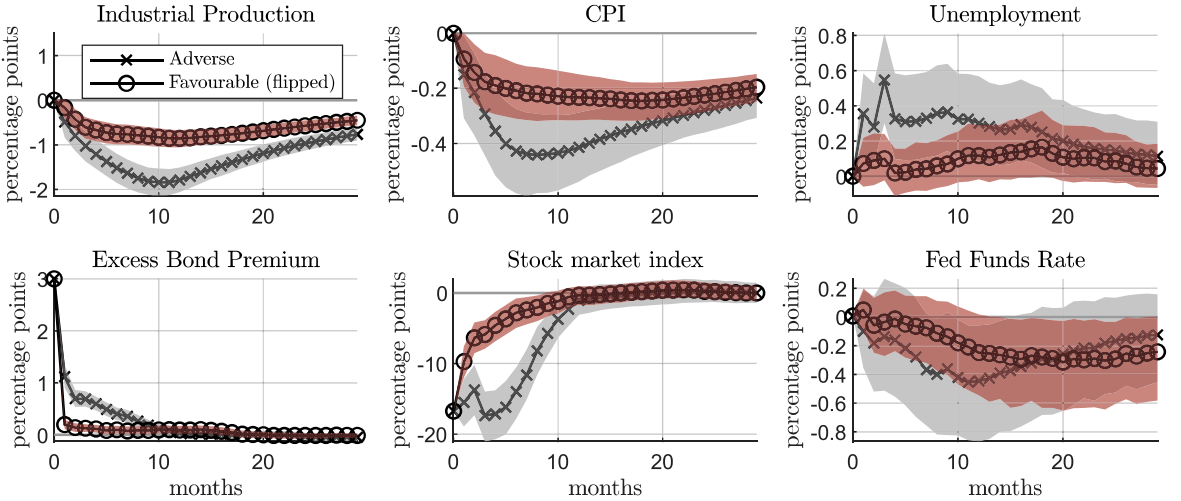
the response of CPI is more pronounced to a favourable shock than to an adverse shock. We acknowledge a short-lived puzzling response of the federal funds rate after a favourable shock, an effect that only lasts one month.

Figure 8 shows that things change considerably when the size of the shock is larger.

Figure 9: Nonlinear effects of financial shocks - Large shock, adverse versus favourable
 A) Pre-Covid sample, 1973M1-2020M2



B) Post-Covid sample, 1973M1-2024M12

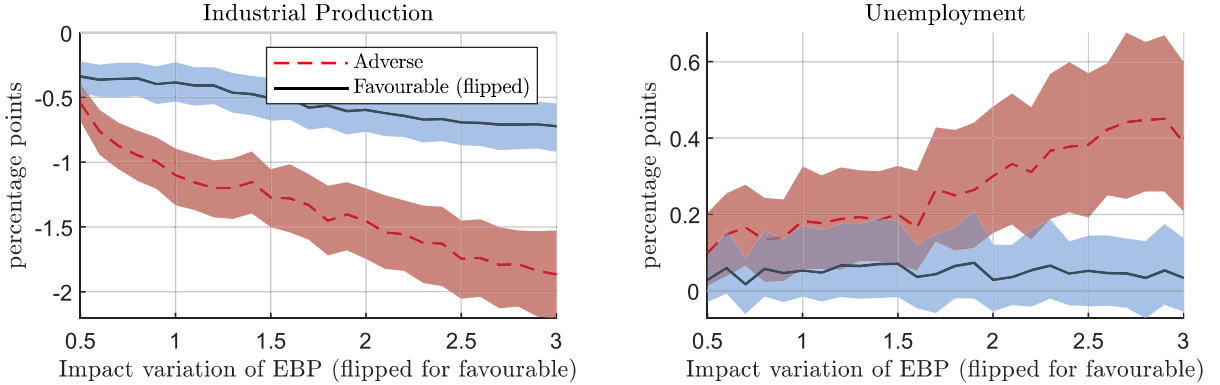


Note: Response to adverse and favourable financial shocks that change the excess bond premium by 50 basis points (top panel) or 300 basis points (bottom panel). The response to favourable shocks has been multiplied by -1 for the purpose of comparison. The lines and bands reported are the pointwise median and 90% coverage bands, respectively.

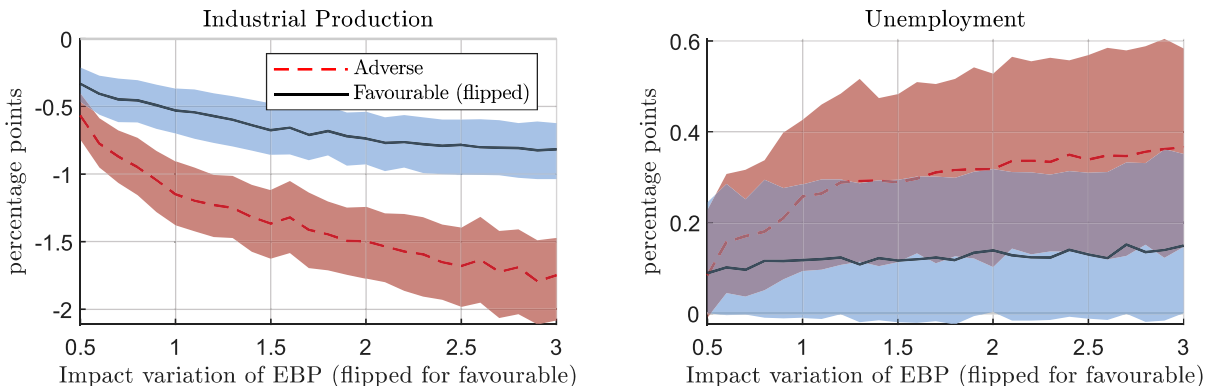
Consider first the results before Covid. In response to an exogenous variation of the excess bond premium by 300 basis points the stock market responds three times as strongly in response to an adverse shock, which also generates a much more persistent effect on the excess bond premium. This results in a considerably stronger effect on

Figure 10: Nonlinear effects of financial shocks

A) Pre-Covid sample, 1973M1-2020M2



B) Post-Covid sample, 1973M1-2024M12



Note: Strongest response within two years from the shock. The horizontal axis reports the impact variation of the excess bond premium, from a minimum of 50 basis points to a maximum of 300 basis points. The response to favourable shocks has been multiplied by -1 for the purpose of comparison, and the corresponding shock should be viewed as a decrease (rather than an increase) in the excess bond premium. The lines and bands reported are the pointwise median and 90% coverage bands, respectively.

industrial production, CPI and unemployment. As an example, the 300 basis point decrease in the excess bond premium only increases industrial production by 0.8%, while the 300 basis point *increase* leads to a maximum drop in industrial production of almost 2%. Consistent with these results, the federal funds rate decreases in response to an adverse shock more than it increases in response to a favourable shock. The results remain robust to the inclusion of the Covid-19 period. The nonlinear effect of

adverse versus favourable shocks is mildly smaller on industrial production, but still present. A non-linearity arises on the response of CPI, which responds more strongly to favourable shocks in the post Covid period.

[Figure 10](#) further inspects the nature of the non-linearity documented in [Figure 8](#)-[Figure 9](#). It shows the response of industrial production and the unemployment rate when the size of the shock is progressively increased to generate impact variations in the excess bond premium of consecutive values from 50 to 300 basis points. For adverse shocks, the figure shows the strongest decrease (for industrial production) and increase (for unemployment) within the first two years from the shock. For favourable shocks the analysis is shown with opposite sign to improve comparability (the underlying shock should be interpreted as decreases rather than increases in the excess bond premium). The figure shows that favourable shocks of a progressively increasing size generate effects that increase in magnitude only mildly. By contrast, adverse shocks of increasing magnitude generate progressively stronger effects.

Broadly speaking, the results documented in [Figure 8](#)-[Figure 10](#) are consistent with Figure 5 from [Forni et al. \(2024\)](#): small adverse and favourable shocks broadly generate symmetric effects, but as the size of the shock increases, adverse shocks affect the real economy much more than favourable ones. However, on closer inspection, two notable differences emerge. First, the results from [Figure 8](#) do not display their puzzling temporary monetary contraction in response to adverse shocks. Second, in [Forni et al. \(2024\)](#) the timing of the maximum effects are similar for positive and negative shock. Our results, instead, document that the size of the shock has a strong effect not only on the size of the responses, but also on their timing. Small shocks generate a maximum effect of unemployment which is mainly concentrated around 16 months from the shock irrespectively of the sign of the shock. By contrast, large shocks imply a much more rapid response to adverse shocks, which generate a peak impact of unemployment already within the first 6 months from the shock. Having relied on the same identification strategies helps us interpret these differences as the result of

not introducing cubic parametric functional constraints in how different non-linearities interact in the model.

Table 1: Splitting variables in the first 6 months from the shock

	IP	CPI	Unemp	EBP	S&P500	Fed funds	sum
IP	20.50%	15.25%	15.75%	16.52%	16.47%	15.52%	100%
CPI	14.43%	26.17%	14.77%	15.07%	14.24%	15.33%	100%
Unemp	15.88%	14.93%	23.09%	14.95%	15.40%	15.75%	100%
EBP	15.36%	15.66%	15.37%	20.90%	16.24%	16.47%	100%
S&P500	15.89%	15.61%	15.05%	17.67%	19.39%	16.39%	100%
Fed funds	14.30%	17.27%	13.30%	13.57%	14.96%	26.60%	100%

Note: Caution should be paid in attaching a structural or economic interpretation to the selection of variables used by BART as splitting variables. The results on how frequently the estimated residuals $w_{t+h}^{(h)}$ featured as splitting variables were omitted to improve visibility.

[Table 1](#) complements the analysis by documenting which variables are used more frequently by BART-LP as splitting variables in the tree structures from the joint posterior distribution. Rows differ depending on which of the size variable is studied as dependent variable. Columns differ for how frequently the corresponding variable in the column is used as a splitting variable, irrespectively of the lag at which it enters the model. As an example, lagged values of industrial production are used as splitting variables around 20% of the times in explaining industrial production, and around 15% of the times in explaining CPI. The table documents that, overall, each variable contributes to explaining mainly the non-linearities on itself, rather than on other variables (we caution against attaching a structural interpretation to the information provided in [Table 1](#)).

[Figure E.9](#) in the Online Appendix shows evidence of time-variation in the effect of financial shocks. It reports the effect of financial shocks on industrial production when varying the initial conditions used to compute the GIRFs. These initial conditions are set equal to the average value of the variables on a rolling window, starting from the beginning of the sample and incrementing it with increments of 12 months. Consistent with the results discussed in this section, adverse shocks have a larger average impact on industrial production. We find evidence that favorable financial shocks can have larger effects on real activity during recessions.

4.2 The non-linear effects of monetary shocks

Monetary policy is known to be an important tool in the tool-kit of policy makers. For this reason, effort has been given to inspect if monetary policy shocks are still effective during economic recessions, which are periods in which monetary policy might be needed the most to sustain economic activity. [Weise \(1999\)](#) and [Tenreyro and Thwaites \(2016\)](#) document opposite results on this matter, finding that monetary policy shocks are more effective during economic recessions (the former) or during economic expansions (the latter). Both contributions use parametric models that only explicitly model the non-linearity over the state of the business cycle. We revisit their analysis using BART-LP in order to jointly study multiple non-linearities within the same framework, namely over the business cycle, as well as over the sign and size of the shock. We then use BART to inspect if Covid-19 has changed the transmission mechanism of monetary policy shocks and altered any non-linearities detected before the pandemic.

We set y_{t+h} from equation (1) equal to six possible variables: (1) the monetary policy shock proxy of [Jarociński and Karadi \(2020\)](#), (2) the one-year government bond yield, (3) real GDP growth, (4) GDP deflator inflation, (5) stock returns, (6) the excess bond premium. The data is monthly, with the pre-Covid sample running from 1979M7 to 2020M2, and the post-Covid sample running up to 2024M12. We include 12 lags in the model. The identification strategy is selected to make the analysis as close as possible to [Jarociński and Karadi \(2020\)](#). We estimate a preliminary linear VAR model using the recursive identification strategy for the first shock, which is the shock to the monetary policy instrument. As in the application to financial shocks, this strategy allows for the calibration of a shock such that the interest rate changes on impact by a selected magnitude of interest. We estimate the response to positive and negative shocks of varying magnitudes that change the interest rate by a minimum of 10 basis to a maximum of 100 basis points. We estimate these impulse responses

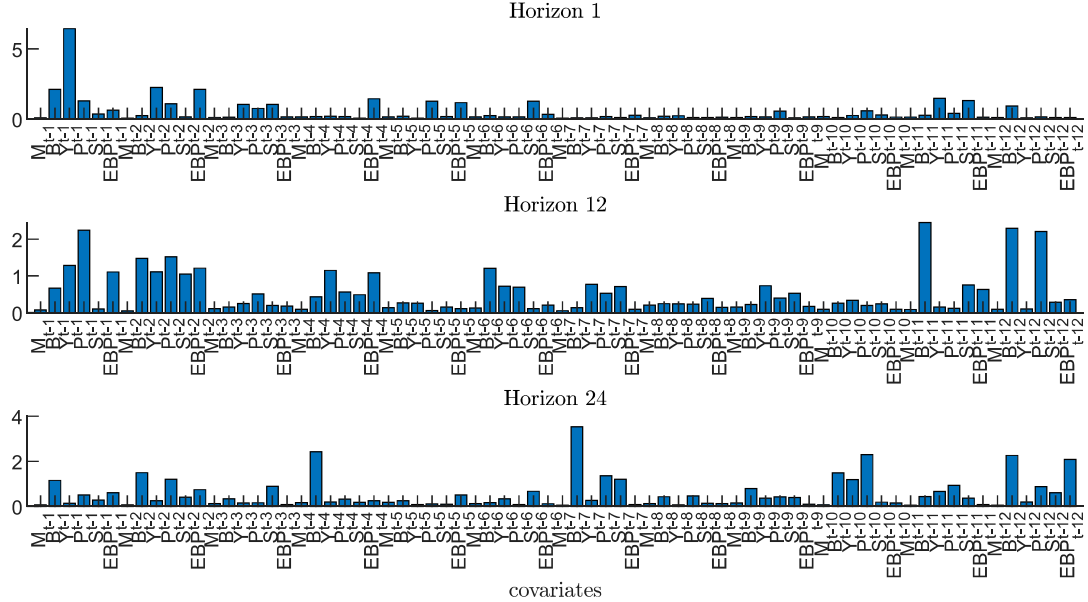
conditioning on being in a recession or and expansion.⁹ We set the number of trees to 500 and use 4,000 posterior draws, with a burn-in of 2,000 draws. The code takes approximately one hour to run to generate 4,000 posterior draws.

Figure 11 shows how frequently, on average, each regressor is used as a splitting variable for each estimated model. The top figure shows the results for the pre-Covid period, while the lower period refers to the full sample. For horizon $h = 1$ the most important regressor for the splitting rules before Covid is real GDP growth (Y_{t-1}), indicating the presence of non-linearity associated with the state of the economy. At longer horizons financial variables become more important. For example, at the one year horizon, the lagged one year rate of the interest rate (B_{t-12}) is used most frequently in splitting rules, followed by stock market returns, the interest rate and the excess bond premium at different lags (S_{t-12}, B_{t-1} and EBP_{t-1}). These variables remain important at the two year horizon. After Covid, the nonlinear patterns captured by the splitting variables do change. For instance, (Y_{t-11}) becomes a very important predictor for output at horizon $h = 1$, and many more variables become important at horizon $h = 24$.

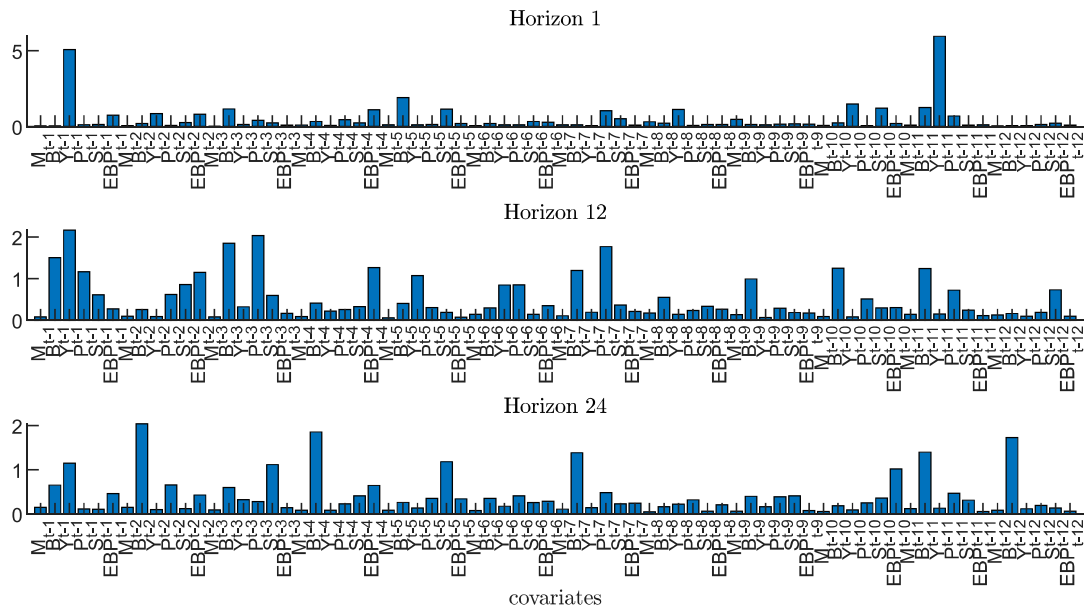
⁹In the case of recessions, we use the initial data from periods when GDP growth is at the following percentiles: 1st, 2.5th, 5th, 10th, 20th. Expansions are defined as being consistent with data from periods when growth equals the 80th, 90th, 95th, 97.5th or the 99th percentile.

Figure 11: Nonlinear effects of monetary shocks

A) Pre-Covid sample, 1979M7-2020M2



B) Post-Covid sample, 1979M7-2024M12



Note: Regressors are indicated as the proxy for the monetary policy (M_t), the one-year government bond yield (B_t), real GDP growth (Y_t), GDP deflator inflation (P_t), stock returns (S_t), and the excess bond premium (EBP_t). Caution should be paid in attaching a structural or economic interpretation to the selection of variables used by BART as splitting variables. The results on how frequently the estimated residuals $w_{t+h}^{(h)}$ featured as splitting variables were omitted to improve visibility.

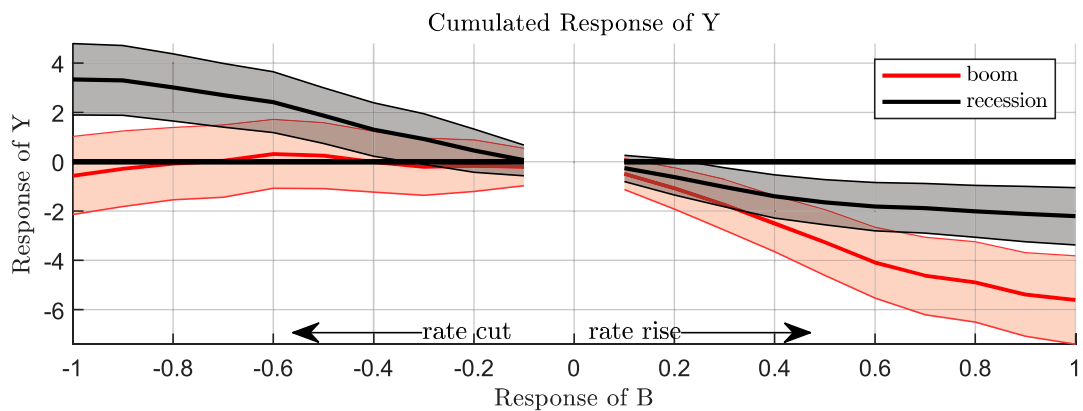
[Figure 12](#) summarises our main result. The figure shows the cumulated response of real GDP growth at the one year horizon to expansionary and contractionary policy shocks. We consider shocks that change the one-year rate by 10 basis points up to 100 basis points with increments of 0.1 percent. Responses conditioned on boom periods are shown in red, while those using recessions as initial conditions are shown in black. The panel above shows the results using data until Covid 19. The panel below uses the full dataset.

The figure suggests that in periods of economic recession, contractionary and expansionary monetary policy shocks generate relatively symmetric effects, both before and after Covid. In addition, as a first approximation, the size of the effect increases proportionately in the size of the underlying shock. The same does not hold when studying periods of economic expansions before Covid. Until 2020M2, in an expansion a contractionary monetary policy shock generates effects of larger magnitude than the corresponding expansionary monetary policy shocks. In an expansion, the effect of contractionary monetary policy shocks increases more than proportionately. All in all, conditioning on contractionary shocks, such shocks used to have a much stronger effect if they hit the economy in a boom than in a recession, while the opposite was true for expansionary shocks.¹⁰ However, we find evidence that the transmission mechanism of monetary policy has changed after Covid 19, in that the nonlinearity is lost. We present impulse responses of all variables in [Figure 13](#). Before Covid, the effect of a contractionary monetary shock on GDP growth is larger and more persistent, but the effect is subdued following the pandemic.

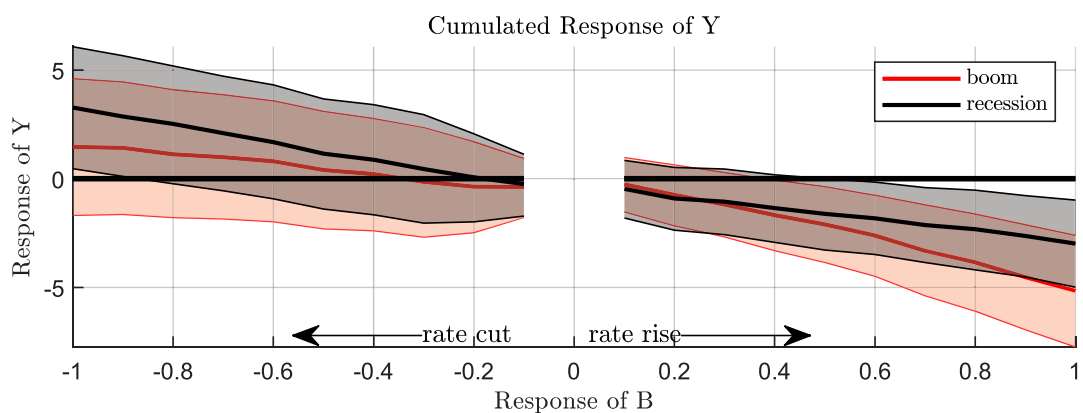
¹⁰In [Section D](#) of the Online Appendix (see [Figure D.3](#)) we consider responses to contractionary shocks using a standard LP that has different coefficients during expansions and recessions, with the regimes determined exogenously via smooth transition process. Evidence for differences in the impact across recessions and booms is less clear-cut in this model. This points to the key advantages of the proposed LP in that it does not rely on an assumed functional form, specific switching variables or regime switching that is independent of the shocks.

Figure 12: Nonlinear effects of monetary shocks

A) Pre-Covid sample, 1979M7-2020M2



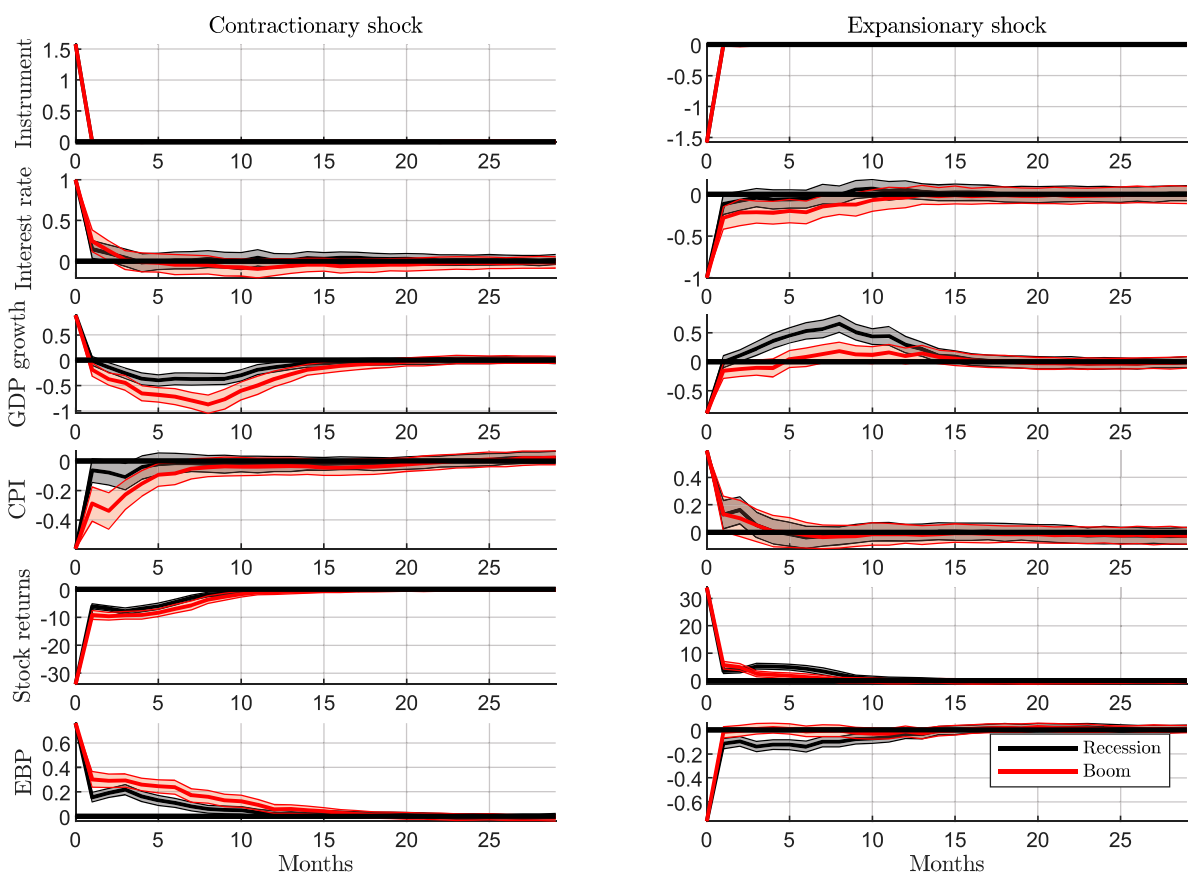
B) Post-Covid sample, 1979M7-2024M12



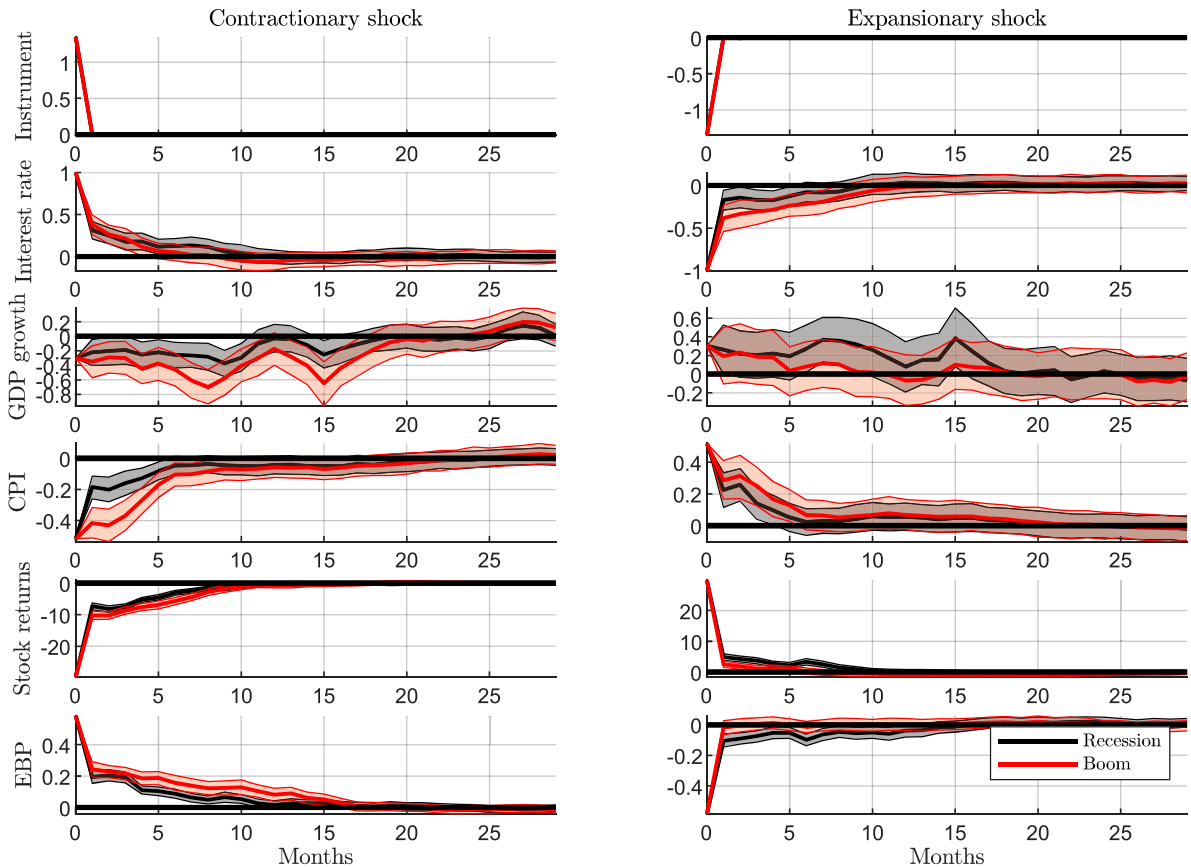
Note: The cumulated response of GDP growth at the one year horizon. Solid lines and shaded areas are the medians and 68% error band of the response from the flexible LP. The dotted lines represent the impact of the shock as it is linearly scaled up.

Figure 13: Nonlinear effects of monetary shocks

A) Pre-Covid sample, 1979M7-2020M2



B) Post-Covid sample, 1979M7-2024M12



Note: Monetary policy shocks calibrated to generate an impact variation of the interest rate of 100 basis points.

The results from [Figure 12](#) help clarify the apparently contradicting results documented by [Weise \(1999\)](#) and [Tenreyro and Thwaites \(2016\)](#). By construction, the smooth transition LP model used by [Tenreyro and Thwaites \(2016\)](#) generates responses that are symmetric when comparing contractionary and expansionary shocks. Similarly, shocks of increasing size cannot generate impulse responses of a different shape within their model. While these two limitations are not present in the smooth transition VAR model used by [Weise \(1999\)](#), its main focus is to inspect a non-linearity over the business cycle, rather than over the size and sign of the shock. Our framework helps investigate the results by [Weise \(1999\)](#) and [Tenreyro and Thwaites \(2016\)](#) when multiple non-linearities are studied at the same time. For contractionary shocks, the main result by [Tenreyro and Thwaites \(2016\)](#) is clearly supported by [Figure 12](#) for the pre-Covid period, as shocks generated in an economic expansion are more effective than in economic recessions. By contrast, for expansionary shocks, there is evidence supporting the finding by [Weise \(1999\)](#) that the effects are stronger in recession rather than in expansion. However, we document that both non-linearities might have been lost in the aftermath of Covid-19. We stress that the post pandemic period is very short, and caution is warranted in drawing conclusions about whether pre-pandemic non-linearities might still be at play.

The main findings documented for monetary contractions before Covid are broadly consistent with [Bruns and Piffer \(2023\)](#), who also use a model for non-linearities over the business cycle, but not formally model dependency over the sign and size of the shock, and use pre-Covid data. [Barnichon and Matthes \(2018\)](#) adjust their FAIR methodology to study non-linear effects of monetary policy shocks depending on the size of the shock. While they do not contemporaneously study non-linearities over the size of the shock nor over the business cycle, their results are consistent with our pre-Covid finding from [Figure 12](#), namely that, before Covid, contractionary shocks were more effective than expansionary shocks. We find that this result used to hold mainly when the shock hits the economy in an economic expansion.

5 Conclusions

Local projections are widely used in Macroeconometrics, as they provide a flexible tool to estimate impulse responses to structural shocks of interest. However, the most popular linear specification of local projections introduces the assumption of a linear relationship among variables within each horizon h considered. This paper introduces a flexible local projection that generalises the model of [Jordà \(2005\)](#) to a non-parametric setting by using Bayesian Additive Regression Trees (BART). Using Monte Carlo experiments, we show that the model is able to capture impulse response non-linearities driven by state-dependence, sign-dependence or size-dependence.

We apply our methodology to US financial and monetary shocks. We complement the results by [Forni et al. \(2024\)](#) on financial shocks. We find further evidence of their result that the effect of adverse financial shocks increases more than proportionately in the size of the shock. At the same time we find that also the timing of the effect changes, as adverse shocks of higher magnitude affect the economy more rapidly. The results also hold when adding post-Covid data to the analysis. We then apply BART-LP to monetary shocks. We find that, before Covid, when contractionary shocks are considered, the results are consistent with the finding by [Tenreyro and Thwaites \(2016\)](#), in that monetary policy is more effective during economic expansions. Yet, in response to expansionary shocks, we find mild evidence in favour of the opposite result before Covid, as documented instead by [Weise \(1999\)](#). The nonlinearity is partly lost when adding Covid to the analysis.

References

- Alessandri, P., Jordà, Ò. and Venditti, F. (2022), ‘Decomposing the monetary policy multiplier’.
- Alessandri, P. and Mumtaz, H. (2017), ‘Financial conditions and density forecasts for us output and inflation’, *Review of Economic Dynamics* **24**, 66–78.
- Alloza, M., Gonzalo, J. and Sanz, C. (2025), ‘Dynamic effects of persistent shocks’, *Journal of Applied Econometrics* .
- Alpanda, S., Granziera, E. and Zubairy, S. (2021), ‘State dependence of monetary policy across business, credit and interest rate cycles’, *European Economic Review* **140**, 103936.
- Auerbach, A. J. and Gorodnichenko, Y. (2013a), Fiscal multipliers in recession and expansion, in A. Alesina and F. Giavazzi, eds, ‘Fiscal policy after the financial crisis’, University of Chicago Press, pp. 63–98.
- Auerbach, A. J. and Gorodnichenko, Y. (2013b), ‘Output spillovers from fiscal policy’, *American Economic Review* **103**(3), 141–46.
- Barnichon, R. and Brownlees, C. (2019), ‘Impulse Response Estimation by Smooth Local Projections’, *The Review of Economics and Statistics* **101**(3), 522–530.
- Barnichon, R., Debortoli, D. and Matthes, C. (2022), ‘Understanding the size of the government spending multiplier: It’s in the sign’, *The Review of Economic Studies* **89**(1), 87–117.
- Barnichon, R. and Matthes, C. (2018), ‘Functional approximation of impulse responses’, *Journal of Monetary Economics* **99**, 41–55.

- Barnichon, R., Matthes, C. and Ziegenbein, A. (2022), ‘Are the effects of financial market disruptions big or small?’, *Review of Economics and Statistics* **104**(3), 557–570.
- Breitung, J. and Brüggemann, R. (2023), ‘Projection estimators for structural impulse responses’, *Oxford Bulletin of Economics and Statistics* **85**(6), 1320–1340.
- Brunn, M. and Lütkepohl, H. (2022), ‘Comparison of local projection estimators for proxy vector autoregressions’, *Journal of Economic Dynamics and Control* **134**, 104277.
- Brunn, M. and Piffer, M. (2023), ‘Tractable bayesian estimation of smooth transition vector autoregressive models’, *The Econometrics Journal* .
- Cascaldi-Garcia, D. (2022), ‘Pandemic priors’.
- Castelnuovo, E. and Pellegrino, G. (2018), ‘Uncertainty-dependent effects of monetary policy shocks: A New-Keynesian interpretation’, *Journal of Economic Dynamics and Control* **93**, 277–296.
- Chipman, H. A., George, E. I. and McCulloch, R. E. (2010), ‘BART: Bayesian additive regression trees’, *The Annals of Applied Statistics* **4**(1), 266–298.
- Clark, T. E., Huber, F., Koop, G., Marcellino, M. and Pfarrhofer, M. (2023), ‘Tail forecasting with multivariate Bayesian additive regression trees’, *International Economic Review* **64**(3), 979–1022.
- Dinh, V. H., Nibbering, D. and Wong, B. (2024), ‘Random subspace local projections’, *Review of Economics and Statistics* pp. 1–33.
- Ferreira, L. N., Miranda-Agrippino, S. and Ricco, G. (2023a), ‘Bayesian local projections’, *The Review of Economics and Statistics* pp. 1–45.

- Ferreira, L. N., Miranda-Agrippino, S. and Ricco, G. (2023b), ‘Bayesian local projections’, *The Review of Economics and Statistics* pp. 1–45.
- Forni, M. and Gambetti, L. (2014), ‘Sufficient information in structural vars’, *Journal of Monetary Economics* **66**, 124–136.
- URL:** <https://www.sciencedirect.com/science/article/pii/S0304393214000634>
- Forni, M., Gambetti, L., Maffei-Faccioli, N. and Sala, L. (2024), ‘Nonlinear transmission of financial shocks: Some new evidence’, *Journal of Money, Credit and Banking* **56**(1), 5–33.
- Gilchrist, S. and Zakrajšek, E. (2012), ‘Credit spreads and business cycle fluctuations’, *American Economic Review* **102**(4), 1692–1720.
- Gonçalves, S., Herrera, A. M., Kilian, L. and Pesavento, E. (2022), ‘When do state-dependent local projections work?’.
- Goulet Coulombe, P. (2024), ‘The macroeconomy as a random forest’, *Journal of Applied Econometrics* **39**(3), 401–421.
- Herbst, E. P. and Johannsen, B. K. (2024), ‘Bias in local projections’, *Journal of Econometrics* **240**(1), 105655.
- Hill, J., Linero, A. and Murray, J. (2020), ‘Bayesian additive regression trees: A review and look forward’, *Annual Review of Statistics and Its Application* **7**(1), 251–278.
- Ho, P., Lubik, T. A. and Matthes, C. (2024), ‘Averaging impulse responses using prediction pools’, *Journal of Monetary Economics* p. 103571.
- Huber, F., Koop, G., Onorante, L., Pfarrhofer, M. and Schreiner, J. (2023), ‘Nowcasting in a pandemic using non-parametric mixed frequency VARs’, *Journal of Econometrics* **232**(1), 52–69.

- Huber, F. and Rossini, L. (2022), ‘Inference in bayesian additive vector autoregressive tree models’, *The Annals of Applied Statistics* **16**(1), 104–123.
- Inoue, A., Rossi, B. and Wang, Y. (2024), ‘Local projections in unstable environments’, *Journal of Econometrics* **244**(2), 105726.
- Jarociński, M. and Karadi, P. (2020), ‘Deconstructing monetary policy surprises: the role of information shocks’, *American Economic Journal: Macroeconomics* **12**(2), 1–43.
- Jordà, Ò. (2005), ‘Estimation and inference of impulse responses by local projections’, *American Economic Review* **95**(1), 161–182.
- Kilian, L. and Kim, Y. J. (2011), ‘How reliable are local projection estimators of impulse responses?’, *Review of Economics and Statistics* **93**(4), 1460–1466.
- Koop, G., Pesaran, M. H. and Potter, S. M. (1996), ‘Impulse response analysis in nonlinear multivariate models’, *Journal of Econometrics* **74**(1), 119–147.
- Lenza, M. and Primiceri, G. E. (2022), ‘How to estimate a vector autoregression after march 2020’, *Journal of Applied Econometrics* **37**(4), 688–699.
- Li, D., Plagborg-Møller, M. and Wolf, C. K. (2024), ‘Local projections vs. vars: Lessons from thousands of dgps’, *Journal of Econometrics* **244**(2), 105722.
- Lusompa, A. (2023), ‘Local projections, autocorrelation, and efficiency’, *Quantitative Economics* **14**(4), 1199–1220.
- Montiel Olea, J. L. and Plagborg-Møller, M. (2021), ‘Local projection inference is simpler and more robust than you think’, *Econometrica* **89**(4), 1789–1823.
- Paranhos, L. (2022), ‘How do firms’ financial conditions influence the transmission of monetary policy? A non-parametric perspective’.

- Plagborg-Møller, M. and Wolf, C. K. (2021), ‘Local Projections and VARs Estimate the Same Impulse Responses’, *Econometrica* **89**(2), 955–980.
- Prüser, J. (2019), ‘Forecasting with many predictors using bayesian additive regression trees’, *Journal of Forecasting* **38**(7), 621–631.
- Ramey, V. A. and Zubairy, S. (2018), ‘Government spending multipliers in good times and in bad: Evidence from US historical data’, *Journal of Political Economy* **126**(2), 850–901.
- Romer, C. D. and Romer, D. H. (2017), ‘New evidence on the aftermath of financial crises in advanced countries’, *American Economic Review* **107**(10), 3072–3118.
- Ruisi, G. (2019), ‘Time-Varying Local Projections’, (891).
- Stock, J. H. and Watson, M. W. (2018), ‘Identification and estimation of dynamic causal effects in macroeconomics using external instruments’, *The Economic Journal* **128**(610), 917–948.
- Tenreyro, S. and Thwaites, G. (2016), ‘Pushing on a string: US monetary policy is less powerful in recessions’, *American Economic Journal: Macroeconomics* **8**(4), 43–74.
- Weise, C. L. (1999), ‘The asymmetric effects of monetary policy: A nonlinear vector autoregression approach’, *Journal of Money, Credit and Banking* **31**(1), 85–108.